Journal of the Taiwan Institute of Chemical Engineers 165 (2024) 105700

Contents lists available at ScienceDirect

Journal of the Taiwan Institute of Chemical Engineers

journal homepage: www.journals.elsevier.com/journal-of-the-taiwan-institute-of-chemical-engineers

The catalytic deoxygenation reaction temperature and N_2 gas flow rate influence the conversion of soybean fatty acids into Green Diesel

R.S.R.M. Hafriz [a,b,*], S.H. Habib [b], N.A. Raof [c], S.Z. Razali [d], R. Yunus [a], N.M. Razali [b], A. Salmiaton [a,e,*]

[a] Department of Chemical and Environmental Engineering, Faculty of Engineering, Universiti Putra Malaysia, 43400 UPM Serdang, Selangor, Malaysia
[b] AAIBE Chair of Renewable Energy, Institute of Sustainable Energy, Universiti Tenaga Nasional, 43000 Kajang, Selangor, Malaysia
[c] Chemical Engineering Department, Faculty of Engineering, Universiti Teknologi Petronas, 32610 Seri Iskandar, Perak, Malaysia
[d] Institute of Nanoscience and Nanotechnology (ION2), Universiti Putra Malaysia, 43400 Serdang, Selangor, Malaysia
[e] Sustainable Process Engineering Research Centre, Faculty of Engineering, Universiti Putra Malaysia, 43000 UPM Serdang, Selangor, Malaysia

ARTICLE INFO

Keywords:
Green diesel
Soybean oil
NiO-calcined dolomite
Catalytic deoxygenation
LCCA

ABSTRACT

Background: Green diesel is a promising alternative as a petroleum replacement given the worldwide demand for petroleum fuel. Environmental issues have drawn public attention and concerns towards advancing renewable energy development. A catalytic deoxygenation (deCOx) was carried out to produce green diesel from soybean oil (SO) using a low-cost NiO-doped calcined dolomite (NiO—CD) catalyst.
Method: The structure, chemical composition and morphology of NiO—CD were comprehensively characterized by XRF, BET, TPD-CO_2, SEM and TEM. In this study, the effect of two operating parameters, reaction temperature and flow rate of nitrogen, was discovered using a one-factor-at-a-time (OFAT) optimisation study. In addition, the life cycle cost analysis (LCCA) of stepwise catalyst preparation and green diesel production has been performed.
Significant findings: An optimal reaction temperature of 420 °C was found to provide the highest yield of green diesel (47.13 wt.%) with an 83.51% hydrocarbon composition. The ideal nitrogen flow rate, however, was found to be 50 cm^3/min, which produced 41.80 wt.% of green diesel with an 88.63% hydrocarbon composition. The deoxygenation reaction was significantly impacted by both reaction temperature and nitrogen flow rate. According to LCCA, NiO—CD catalyst has potential to lower the overall cost of producing green diesel compared to commercial zeolite catalysts.

1. Introduction

In recent years, the ongoing effort to achieve carbon net zero by 2050 has boosted the development of green diesel production. Industry 4.0 is shifting away from energy derived from fossil fuels to mitigate the climate change effect on a global scale [1]. Notably, the performance and utilization of fossil fuels are difficult to match. Consequently, it is inevitable to eliminate its production and usage. By 2035, the International Energy Agency (IEA) predicted the utilization of petroleum-based fuels for energy generation will increase because of rising energy demand, thus sparking concerns about global greenhouse gas (GHG) emissions that lead to changes in climatic conditions [2]. Owning to the current impact of fossil fuels on climate scenarios and energy demands, numerous works have been researched and developed to produce green diesel from biobased resources with matching properties as a possible replacement for fossil fuels [3–5].

A sustainable and commercial-scale biofuel production process in any country will undergo certain evaluation criteria, which the selection of the right biofuel feedstock is the first step. Researchers are trying to identify the most efficient (in terms of emission characteristics, engine performance, and combustion behavior) and effective (conversion rate and higher oil content) biofuel feedstocks among both edible and non-edible oils [6]. Various methods of cracking the long carbon chain of triglyceride in the different feedstock of vegetable oil into shorter carbon chains have been adapted extensively to produce green diesel. Kuan et al. [7] used thermal transformation to obtain green diesel in diesel and kerosene range from palm methyl ester. Meanwhile, Haryani et al. [8] use the same feedstock to produce green diesel through the catalytic

* Corresponding authors.
E-mail addresses: raja.hafriz@uniten.edu.my (R.S.R.M. Hafriz), mie@upm.edu.my (A. Salmiaton).

https://doi.org/10.1016/j.jtice.2024.105700
Received 14 May 2024; Received in revised form 18 July 2024; Accepted 7 August 2024
Available online 26 August 2024

cracking method. The study successfully achieved 88.7% conversion of palm methyl ester into liquid fuel. A similar approach to the catalytic cracking method was used by Neonufa et al. [9] to convert palm kernel methyl ester into jet fuel. Several other studies also reported that catalytic cracking of triglycerides from jatropha curcas, rapeseed oil and soybean oil has shown a promising outcome in obtaining green diesel with diesel and kerosene range [10–12]. Among these catalytic cracking methods, catalytic deoxygenation, hydrogenation, and hydro-deoxygenation are proven to maximize the conversion of triglycerides into green diesel [13,14]. Generally, catalytic hydrogenation and hydro-deoxygenation mechanisms occur in catalytic deoxygenation (deCOx), where the first step to breaking a triglycerides olefinic bond into a saturated C—C bond is by introducing a hydrogen atom from the feedstock itself [15]. This mechanism is followed by C—O linkage scission as the precursor to decarbonylation, decarboxylation and hydro-deoxygenation pathways where water commonly becomes the by-product [16]. The extraction of oxygenated compounds from bio-oil chemical structures through these pathways produces hydrocarbons, which can be denoted as green diesel.

The selection of a catalyst is paramount to obtain the deoxygenation (deCOx) pathways. Metal oxides and commercial zeolite-based catalysts are often selected in this reaction due to their high selectivity towards deoxygenation pathways [17–19]. These studies reported that the acidity properties and mesoporous structure of synthesized catalyst induced the deoxygenation pathways. The high acidity properties come from hydrogen transfer from the feedstock that aids in the conversion of aldehyde intermediate into hydrocarbon [20]. Concurrently, the mesoporous size structure of the catalyst support improves the selectivity of the mechanism involving unstable oxygenated compounds [21]. As a result, high hydrocarbon content was obtained in green diesel. In this reaction, temperature and its environment play a major role in identifying the quantity and quality of the green diesel produced. A detailed review by Cheah et al. [16] stated that the suitable deoxygenation reaction temperature to produce high-quality and yield green diesel is between 300 and 380 °C in an inert atmosphere with the presence of metal oxides, zeolites and mesoporous catalysts. The review also suggested that these two parameters are important in determining the desired properties of green diesel production.

Other than zeolites, metal oxides, and mesoporous catalysts, natural basic catalyst support is a good alternative to commercial catalysts. Base catalyst support such as layered double hydroxides (LDH), activated carbon and calcium oxide catalysts has a good selectivity towards deoxygenation reaction [22–24]. Moreover, in recent years, a basic low-cost catalyst namely dolomite has garnered attention in green diesel production through catalytic deoxygenation. Ali et al. [25] successfully generated green diesel with 58% of palm oil sludge conversion using a dolomite catalyst while Buyang et al. [26] successfully produced 68% of waste cooking oil-based green diesel using a dolomite catalyst. These two studies proved that a low-cost dolomite catalyst is a good alternative catalyst in converting triglycerides-based feedstock via catalytic deoxygenation (deCOx) into green diesel. However, due to its unfamiliar status in this catalytic deoxygenation (deCOx) reaction, there is an immense lack of study on the reaction parameters via OFAT to produce green diesel from soybean oil using low-cost, NiO-dolomite catalysts as potential deoxygenation catalyst. As mentioned earlier, the reaction temperature and nitrogen flow rate will steer the results of green diesel produced on the quality and yield. Hence, this experimental work aims to examine the effect of temperature reaction and flow rate of nitrogen gas in SO-based green diesel composition via the catalytic deoxygenation (deCOx) using a low-cost modified dolomite catalyst. The data obtained from this work is essential in the contribution to the knowledge pool. Additionally, a life cycle cost analysis (LCCA) of stepwise catalyst synthesized and green diesel production was performed. LCCA has the potential to serve as an indicator for assessing the progress of the green diesel sector. Besides that, a comparison of the LCCA of a heterogeneous catalyst, NiO—CD and a commercial zeolite catalyst has been carried out for the production of green diesel.

2. Experimental

2.1. Materials

The reagents in this experimental work were purchased and used without further purification. Systerm Chemicals Sdn. Bhd. provided analytical grade metal nitrate salts, specifically 99.8% purify of nickel (II) nitrate, $Ni(NO_3)_2{\cdot}6H_2O$. Northern Dolomite Sdn. Bhd., Perlis, North Malaysia, supplied the low-cost Malaysian Dolomite used as a supported catalyst. Industrial nitrogen gas (N_2) with a purity of 98% and n-hexane with a purity of > 98% (for GC–MS analysis) were provided by Biogas Sdn. Bhd. and Sigma Aldrich, respectively. Scomi Energy Services Bhd supplied the soybean oil (SO) feedstock, which contained 99.6% oxygenated compounds. Table 1 shows the main constituents of soybean oil (SO) as determined by Gas Chromatography-Mass Spectrometry (GC–MS) analysis. The predominant composition observed in SO was fatty acid with 83.6% followed by furan (5.7%) and other compositions (10.7%), including ester, aldehyde, siloxane and siloxane. Furan compounds (5.7%) have been discovered and detected in soybean oil due to heat processing or prolonged storage. These chemicals are commonly produced by the oxidation of fatty acids and triglycerides. According to Xiao *et al.* [27], heating soybean oil leads to the production of volatile substances such as aldehydes, alcohols, ketones, and furans. Elevated temperatures result in a more noticeable release of undesirable compounds. This aligns with research conducted by Fan et al. [28]; it was discovered that soybean oil could generate furans when subjected to heat processing at a temperature of 120 °C for 25 min or when stored for an extended period at a temperature of 25 °C. Oleic acid accounts for 40.1% of this soybean oil's monounsaturated fatty acid composition, followed by palmitic acid (29.4%) and stearic acid (14.1%), both of which are saturated fatty acids. The existence of this prominent fatty acid has been determined and verified through the investigation undertaken by Livia et al. [29], Souza et al. [30], and Dona et al. [31].

2.2. Synthesis, characterization & LCCA of NiO-CD catalyst

2.2.1. Thermal activation of dolomite catalyst

The dolomite powder was subjected to 250 in ASTM Ell using a Retsch Test Sieve. Prior to this sieving process, the stone form of dolomite was crushed and ground into a specific fine powder. The sieved and fine dolomite powder was calcined in an air environment in a horizontal tube furnace with a heating rate of 10 °C/min. The calcination temperature of dolomite powder was kept at 900 °C for 4 h before being brought down to room temperature.

2.2.2. Synthesis of 5 wt.% of NiO-calcined dolomite (NiO—CD) catalyst

The liquid-liquid blending known as the precipitation technique was used to create the modified dolomite catalyst. To begin, 50 g of fine calcined dolomite (CD) was dispersed in 100 ml of deionized water for 10 min at 60 °C while being constantly stirred. 5 wt.% or 2.5 g of nickel (II) nitrate was totally dissolved in deionized water (10 ml) before being dropped into the CD suspension and stirred for 4 h at 400 rpm at 60 °C. The resulting sludge-like catalyst was dried overnight in an oven with a temperature of 120 °C. Prior to characterization, the ground and sieved

Table 1
Soybean oil's composition from GC–MS analysis.

Compositions	Percentage (%)
Palmitic acid (Hexadecanoic acid), $C_{16}H_{32}O_2$, C16:0	29.4
Stearic acid (Octadecanoic acid), $C_{18}H_{36}O_2$, C18:0	14.1
Oleic acid (cis-9-Octadecanoic acid), $C_{18}H_{34}O_2$, C18:1	40.1
Furan	5.7
Others (ester, aldehyde, siloxane, etc.)	10.7

modified dolomite catalyst was calcined in a horizontal tube furnace for 4 h at 900 °C with a heating rate of 10 °C/min.

2.2.3. Catalyst characterization

Through nitrogen isotherm adsorption-desorption analysis, the pore volume, average pore size, and surface area distribution of the synthesized dolomite catalysts were determined using a Brunauer-Emmett-Teller (BET) method. An adsorption/desorption analyzer (model: Thermo-Finnigan Sorpmatic 1990 series) was used for the measurement. Prior to the measurement, the catalysts were degassed at 150 °C overnight to eliminate the moisture and other adsorbed gases from the synthesized dolomite catalyst surfaces. The processes of N_2 adsorption and desorption on the synthesized dolomite catalyst surfaces were carried out at a temperature of 196 °C in a vacuum chamber. Using wavelength dispersive X-ray fluorescence (WDXXRF; model Bruker, S8 TIGER), the chemical composition of CD and NiO—CD catalyst was evaluated and identified. The basic properties of the synthesized dolomite catalyst were identified using CO_2 temperature-programmed desorption (TPD). This basicity strength measurement of the synthesized catalyst was performed using a Thermo Finnigan TPD/R/O 1100 instrument from Thermo Fisher Scientific equipped with a thermal conductivity detector (TCD) and CO_2 as probe molecules. The analysis test was carried out by inserting 0.05 g of synthesized catalyst into a quartz tube reactor (internal diameter: 6 mm). The synthesized catalysts were pre-treated with nitrogen, N_2 gas flow for 30 min at 250 °C, followed by carbon dioxide, CO_2 for 1 hour gas at ambient temperature to allow adsorption of CO_2 onto the synthesized catalytic surfaces. The excess CO_2 was then removed by purging N_2 gas for 30 min with a flow rate of 20 ml/min. Helium gas was purging at a flow rate of 30 ml min^{-1} from the temperature of 60 to 900 °C, with a 10 °C min^{-1} heating ramp. The basic properties of the synthesized catalyst were evaluated and identified by integrating the area under the given graph of CO_2 desorption. The morphology structure of the synthesized catalysts was evaluated and examined using scanning electron microscopy (SEM) and transmission electron microscopy (TEM) under different magnifications. The high-resolution images of synthesized catalysts were captured using an SEM JOEL 6400 electron microscope at an acceleration voltage of 40 kV and a JEM-2100F field emission electron microscope at an acceleration voltage of 200 kV, respectively.

2.2.4. Life cycle cost analysis (LCCA) of stepwise NiO-CD catalyst preparation

The life cycle cost analysis (LCCA) of stepwise pretreatment and post-treatment of NiO—CD catalyst preparation is shown in Table 2. In this work, the cost estimation for synthesized dolomite catalyst preparation is critical in identifying the feasibility of this procedure to construct for an upscaling means. LCCA emphasises all criteria, from raw material source to catalyst preparation method, necessary treatment process to catalyst reusability. Following the favorable outcome of using a modified Malaysian Dolomite catalyst that yielded higher hydrocarbon composition green diesel, the stepwise NiO—CD catalyst preparation LCCA has great potential as an indicator of how Malaysia's green diesel industry is developing. The LCCA was evaluated based on 1 kg production of NiO—CD catalyst via precipitation technique using 5% nickel dispersion (50 g of $Ni(NO_3)_2{\cdot}6H_2O$). 1 kg production cost of NiO—CD catalyst after the evaluation was RM 33.99 including the running charges which is 10% of the NCC as mentioned in Table 2. This catalyst production cost was compared to the similar stepwise LCCA catalyst preparation of synthesized ZIF-8 MOF-derived CaO/ZnO catalyst by Ruatpuia et al. [32]. The analysis established that the total cost of 1 kg production of ZIF-8 MOF-derived CaO/ZnO was $18.95 (RM 88.79), rounding up to 62% higher than the cost production of synthesized NiO—CD catalyst (RM 33.99) referencing to the similar LCCA approach. In addition, the final cost of 1 kg production of synthesized NiO—CD catalyst for 5 times recyclability and reusability was as low as RM 6.80 per cycle. Conclusively, LCCA with the catalyst's efficient performance and affordability signifies the productivity and the economic impact of the catalytic deoxygenation process on green diesel production. The LCCA calculated cost merely demonstrates the potential to lower the overall cost of green diesel production via catalytic deoxygenation.

Table 2
Life Cycle Cost Analysis (LCCA) of stepwise NiO—CD catalyst preparation.

No.	Step involved	Detail of process	Cost in Malaysia Ringgit (MYR)
1.	Pure Chemical Cost (PCG)	1 kg of NiO derived dolomite = 1000 g of pure dolomite + 50 g of Ni $(NO_3)_2{\cdot}6H_2O$ = RM 0.15 + RM 9.96 = RM 10.11	**RM 10.11**
2.	Catalyst Pre-Treatment Cost (CPTC) a) Sieving process b) Thermal activation of dolomite (calcined dolomite, CD production) – furnace (7000 W)	a) No cost involved b) Utilities: Electricity (7 kW x 4 h = 28 kWh) = 28 kWh x RM 0.1979* = RM 5.54	a) RM 0.00 b) RM 5.54 Total: **RM 5.54**
3.	Catalyst Preparation Cost (CPC) a) Precipitation technique – Hotplate (650 W) b) Drying process – Oven (2700 W) c) Grinding process – Commercial Grinder (3500 W)	a) Utilities: Electricity (0.65 kW x 4 h = 2.6 kWh) = 2.6 kWh x RM 0.1979* = RM 0.51 Utilities: Water (4 h used) = 0.01 m^3 x RM 2.07 **= RM 0.0207 b) Utilities: Electricity (2.7 kW x 12 h = 32.4 kWh) = 32.4 kWh x RM 0.1979* = RM 6.41 c) Utilities: Electricity (3.5 kW x 4 h = 14 kWh) = 14 kWh x RM 0.1979* = RM 2.77	a) RM 0.51 + RM 0.0207 = RM 0.53 b) RM 6.41 c) RM 2.77 Total: **RM 9.71**
4.	Calcination of NiO—CD (CNC) - furnace (7000 W)	Utilities: Electricity (7 Kw x 4 h = 28 kWh) = 28 kWh x RM 0.1979* = RM 5.54	**RM 5.54**
	Net Cost of Catalyst (NCC)	PCG + CPTC + CPC + CNC = RM 10.11 + RM 5.54 + RM 9.71 + RM 5.54 = RM 30.90	**RM 30.90**
	The total cost of 1 kg NiO—CD catalyst	NCC + Running charges (10% of the NCC) = RM30.90 + RM 3.09 = RM 33.99	**RM 33.99**
	The final cost of 1 kg catalyst after 5 times reused	One-time preparation cost/no. of cycles towards the catalyst reusability = RM 33.99 / 5 = RM 6.798	**RM 6.80**

* Electricity tariff provided by Tenaga Nasional Berhad (TNB) Malaysia excluded green electricity tariff by government Malaysia.
** Water tariff for Higher Learning Institutions (HLIs) provided by Air Selangor (State government of Selangor, Malaysia).

2.3. Catalytic deoxygenation (deCOx) of soybean oil (SO)

SO was undergo catalytic deoxygenated in a 1000 mL fractionation catalytic system that was mechanically agitated (Fig. 1).

Typically, 150 g of soybean oil and 5% by weight of NiO—Calcined Dolomite (NiO—CD) catalyst were added to the 1000 ml glass reactor. The glass reactor was flushed with inert gas of N_2 at 100–200 cm^3/min flow rate to remove any remaining oxygen (hydrogen-free condition) and the reaction mixture was constantly stirred at 400 rpm. To reach the desired reaction temperature of 390 ± 10 °C, the reaction will take approximately 18–20 min and 30 min to complete the deoxygenation,

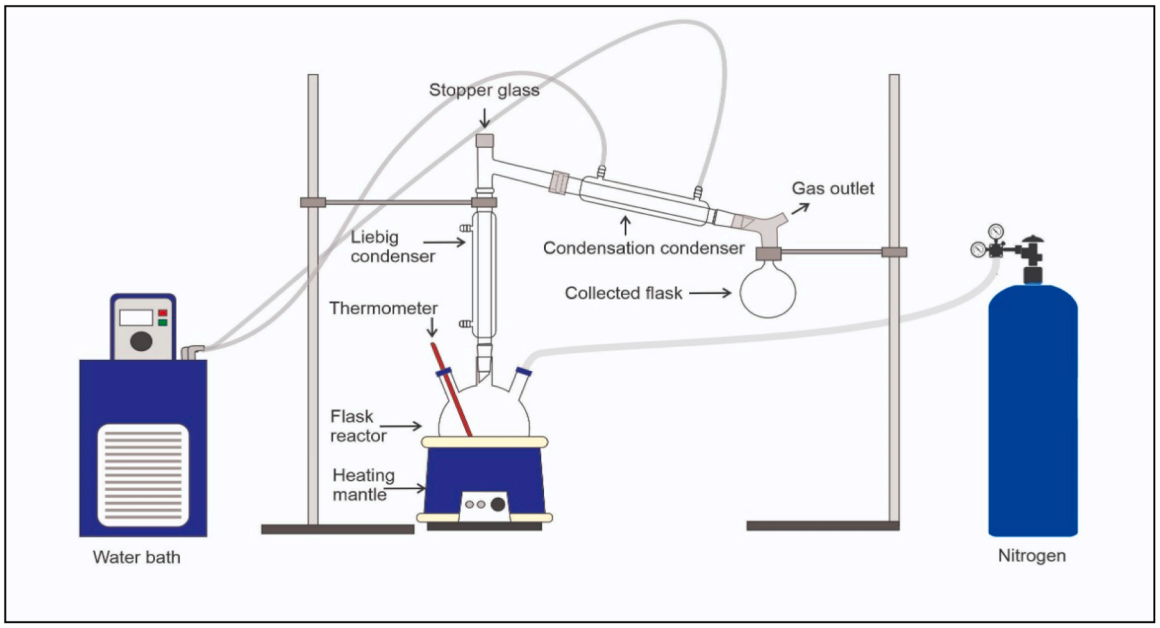

Fig. 1. Fractionated cracking system set up for catalytic deoxygenation reaction.

deCOx reaction. The vapor/volatile product was condensed and collected in the reflux flask. In order to ascertain the distribution of products resulting from the catalytic deoxygenation of SO and the conversion of SO (liquid and gas product), a thorough mass balance has been developed. The weight of the flask reactor and the collected flask before and after the reaction were recorded. The gas release was determined by measuring the weight of coke and catalyst left in the flask reactor, as well as the weight of liquid product generated in the collected flask. The calculation was based on the differences between the initial feedstock, the amount of coke, the mass of the catalyst and the weight of the liquid product. The liquid product in the collection flask contains a mixture of green diesel, acid phase, and soap. The soap formation has been separated and removed using filter paper. The filtration liquid included two distinct phases: green diesel which formed the upper layer, and an acid phase, which formed the bottom layer. The acidic phase was isolated from the green diesel during the decantation process. The final green diesel products were analyzed using GC–MS. Mass balance Eqs. (1) and (2) were used to calculate the product yield and the conversion of SO, respectively [33].

$$Yield\ of\ green\ diesel\ (\%) = \frac{mass\ of\ oil\ green\ diesel(g)}{mass\ of\ Soybean\ Oil\ used\ (g)}\ x\ 100\% \quad (1)$$

$$Conversion\ of\ SO\ (\%) = \frac{mass\ of\ SO\ (g) - mass\ of\ coke\ (g) - mass\ of\ catalyst\ (g)}{mass\ of\ oil\ SO\ (g)}\ x\ 100\% \quad (2)$$

2.4. Product analysis

The green diesel was diluted in n-hexane and quantitatively analyzed in split mode on a Shimadzu GC-14B model of gas chromatography equipped with a ZB-5MS column (30 m length x 0.25 m film thickness x 0.25 mm inner diameter). The initial temperature of the oven was set up to hold for 3 min at 40 °C before ramping up to 300 °C with a heating rate of 7 °C/min and remaining there for 5 min. 250 °C was set up for the injection temperature and Helium acted as carrier gas was used at 3.0 ml/min flow rate. Diffraction peaks from GC–MS spectra of compounds, particularly hydrocarbons (C_8–C_{24}) and unstable oxygenated compounds, were evaluated and identified using the National Institute of Standards and Testing (NIST) library. Although GC–MS analysis does not provide precise quantitative findings for compounds, it is feasible to assess the selectivity and yield of hydrocarbon products by analyzing the peak regions on the chromatograph. The magnitude of a compound's peak area is directly correlated with both its amount and the relative amount of the product [34,35]. To ensure that the findings can be replicated, the tests were conducted three times, and the average values of the peak area and peak area% were calculated. The primary products were identified and distinguished using a probability match of 95 % or above [36]. The Eq. (3) was used to calculate the yield of hydrocarbon (Y) from green diesel produced [37,38].

$$Y = \frac{\sum a_h}{\sum a_p} \times 100\% \quad (3)$$

Where a_h = Area of hydrocarbon compound (C_8–C_{24}), a_p = Total area of the composition product.

The selectivity of hydrocarbon product (S) for green diesel was determined using Eq. (4).

$$S = \frac{\sum a_s}{\sum a_t} \times 100\% \quad (4)$$

Where a_s = Area of the selected hydrocarbon fraction, a_t = Total area of hydrocarbon compounds.

The oxygenated compound removal in percentage was calculated using Eq. (5) [33].

$$\frac{\Sigma \text{ Area of oxygenated compound } (SO) - \Sigma \text{ Area of oxygenated compound } (PO)}{\Sigma \text{ Area of oxygenated compound of } SO} \; x\; 100\% \quad (5)$$

3. Results and discussions

3.1. Physicochemical properties and morphology of the synthesized dolomite catalyst

The X-ray diffraction (XRD) pattern of the synthesized dolomite catalyst after being calcined at a temperature of 900 °C for a duration of 4 h is depicted in Fig. 2(A). The XRD pattern of the CD catalyst primarily consisted of calcium oxide (CaO) and magnesium oxide (MgO). The CaO peaks at 2θ were observed at angles of 32.4°, 37.6°, and 54.1° (JCPDS File: 37–1497). Meanwhile, the MgO peaks were observed at angles of 43.1°, 62.5°, 74.9°, and 78.8° (JCPDS File: 71–1176). These observations are consistent with the findings reported by Zhou *et al.* [39]. The significant intensities of the diffractograms demonstrated the high degree of crystallinity of CaO–MgO. The XRD analysis of NiO-doped dolomite (NiO—CD) catalysts revealed distinct patterns of CaO and MgO. These patterns showed the reflection peaks of CaO and MgO were slightly shifted along with the reduction in the intensity of the CaO-MgO phase peak, indicating the successful dispersion of NiO on the CD catalyst's surface. This discovery aligns with the alteration of the CaO-MgO phase during the introduction of transition metal, as observed by Harith et al. [40] and Shajaratun et al. [41]. Additionally, a new peak corresponding to the crystallization of the NiO at 2θ = 47.58° (JCPDS: 01–042–1300) was observed, distinguishing it from the CD catalyst.

The compositions of synthesized CD and NiO—CD catalysts are shown in Fig. 2(A). According to the XRF measurement, CaO was the major component formed upon decomposition of the CD catalyst, which accounts for 69.3% of the total mass. MgO was the second most abundant component, accounting for 30.2% of the total mass. The trace amount of Fe_2O_3 (0.5%) may have come from raw material impurities or contamination during the analysis. At high-temperature thermal activation (>700 °C), an anhydrous carbonate mineral known as dolomite ($CaMg(CO_3)_2$), composed of calcium magnesium carbonate, was completely decomposed to CaO and MgO [42]. Because of its alkalinity, CaO has the potential as a CO_2 capture absorbent and performs well on cracking heavy compounds into light oxygenated compounds [43,44]. In different studies, CaO assists in deoxygenation and deacidification reactions, reducing the acid value of the pyrolysis oil and favoring the production of biofuel-based hydrocarbons [45–47]. Through aldol condensation and ketonization reactions, MgO catalysts can also effectively decrease the oxygenated content of the produced pyrolysis oil [48]. The XRF analysis of nickel-modified calcined dolomite (NiO—CD) catalysts revealed that major CaO (74.6%) and MgO (20.9%) components were found, too, with a trace amount of NiO (4.1%) and Fe_2O_3 (0.4%). Since 5 wt.% of nickel (II) nitrate was initially used in the reaction, the resulting 4.1% NiO shows successful dispersion of nickel onto the calcined dolomite catalyst. The small addition of nickel oxide, NiO can effectively enhance the quality of pyrolysis oil produced by lowering the C—C degradation energy and therefore boosting the reaction of chain scission [49]. Furthermore, the cracking of C—H bonds naturally requires a significant amount of energy; improvements in catalytic technology [50] and process optimization may lessen these energy requirements, which might lower the running costs of producing green diesel.

CO_2-TPD analysis was used to characterize the basic properties of the catalyst as well as the CO_2 desorption behavior on the synthesized dolomite catalyst surface. The profile of CO_2 desorption and the resultant basicity data are illustrated in Fig. 2**(B)**. Based on Fig. 2**(B)**, both catalysts exhibited strong basicity, which can be denoted by the appearance of desorption peaks at high-temperature regions, 722 °C for CD and 822 °C for the modified catalyst. In addition, a weak peak can be observed at 546 °C for the NiO—CD catalyst graph pattern, with a corresponding amount of CO_2 desorbed of approximately 2.75×10^{20} atoms per gram. These sites exhibit a lower binding energy for CO_2, indicating that the CO_2 molecules are less strongly attached and desorb at lower temperatures. According to Rahman et al. [51], the strength of CO_2 desorption peak-derived temperature was classified as low (250 °C), medium (250 to 500 °C) and high (>500 °C). Based on the basicity data, the modified NiO—CD catalyst exhibited slightly higher basicity than the CD catalyst with 4.40×10^{21} atom/g compared to 1.73×10^{21} atom/g, which was attributed to the basicity properties of alkaline earth dolomite, CaO–MgO.

Fig. 2(D) shows the increased surface area of the synthesized NiO—CD catalyst did not impede or hinder CO_2 accessibility to basic sites on dolomite. According to the theory, the inclusion of NiO species enhances the presence of acidic sites in the catalyst system. However, this study found evidence that contradicts this assertion. The inclusion of NiO has the potential to modify the surface morphology of the dolomite catalyst. Modifications in the surface morphology can impact the distribution and intensity of acidic sites. Besides that, NiO can function as either an electron donor or acceptor, hence influencing the electron density within the dolomite catalyst. The variation in electron density can impact the acid-base characteristics of dolomite, resulting in a decrease in the quantity and strength of acidic sites of NiO—CD catalyst. As reported by Shamsuddin et al. [52], the addition of NiO species to a dolomite support catalyst will result in the synthesis of the catalyst with bifunctional acid-base properties based on TPD-CO_2 and TPD-NH_3 analysis. The addition of NiO promotes both strong acid and basic sites in the catalyst system based on NH_3 and CO_2 desorption results. According to the previous study [53], despite the fact that NiO species presence on the surface of the dolomite support catalyst system will induce strong acidic sites, the modified dolomite catalyst outperforms the calcined dolomite catalyst in terms of base properties. The high percentage dispersion of NiO onto dolomite catalyst resulted in the synergistic effect of NiO—CaO/MgO creating catalysts with bi-functional acid-base properties. This property would allow the catalyst to remove oxygenated species in the production of waste cooking oil-based green diesel via cracking and deoxygenation routes [54].

Fig. 2(C) compares CD and NiO—CD catalyst morphologies using SEM and TEM upon thermal activation at 900 °C. Based on Fig. 2**(C1)**, smaller uniform-size aggregated round-shaped and finer particles were discovered in the SEM image of the CD catalyst. It proves that Malaysian dolomite catalyst, $CaMg(CO_3)_2$ in the form of double carbonate of calcium and magnesium was successfully decomposed to the single metal oxide of CaO and MgO due to the segregation of the individual grain observed in the SEM image of CD catalyst under this temperature of thermal activation. The clear view formation of single metal oxide, CaO and MgO can be observed through a TEM image of a CD catalyst (Fig. 2 **(C2)**) with a cuboid-shaped CaO structure and scattered aggregate or circular-shaped MgO particles that agglomerate near the CaO edges. This discovery was similarly reported by Wang et al. [55], TEM image of the Calcined Dolomite catalyst showed that the blocks appear to consist of CaO as the major component, whereas the small uniform spherical particles with 200 nm of diameter are mostly MgO. According to Hartman *et al.* [56] and Wang *et al.* [57], MgO particles have a greater surface area than CaO particles after calcination due to differences in sintering rates and thermal decomposition kinetics. It has been demonstrated that CaO particles are generally larger than MgO particles

following calcination, mostly because of variations in their thermal breakdown behavior. Based on the SEM image of the NiO—CD catalyst in Fig. 2**(C3)**, a low degree of agglomeration with rough grain segregation morphology was observed due to the nickel metal was successfully dispersed onto the dolomite catalyst surface. According to the study conducted by Hafriz et al. [33], metal incorporation into the CMD900 catalyst interstitial regions was aided by the liquid-liquid blending (precipitation technique) of the CMD900 catalyst solution and metal precursor solution. Furthermore, the successful dispersion of NiO has a significant impact on the CD catalyst morphology, transforming it from a cuboid-circular shape to a spherical structure, as seen in the TEM image of the NiO—CD catalyst in Fig. 2**(C4)**. Under this higher magnification of TEM, the different orientations can be observed due to the interaction of multiple phases or particles such as the

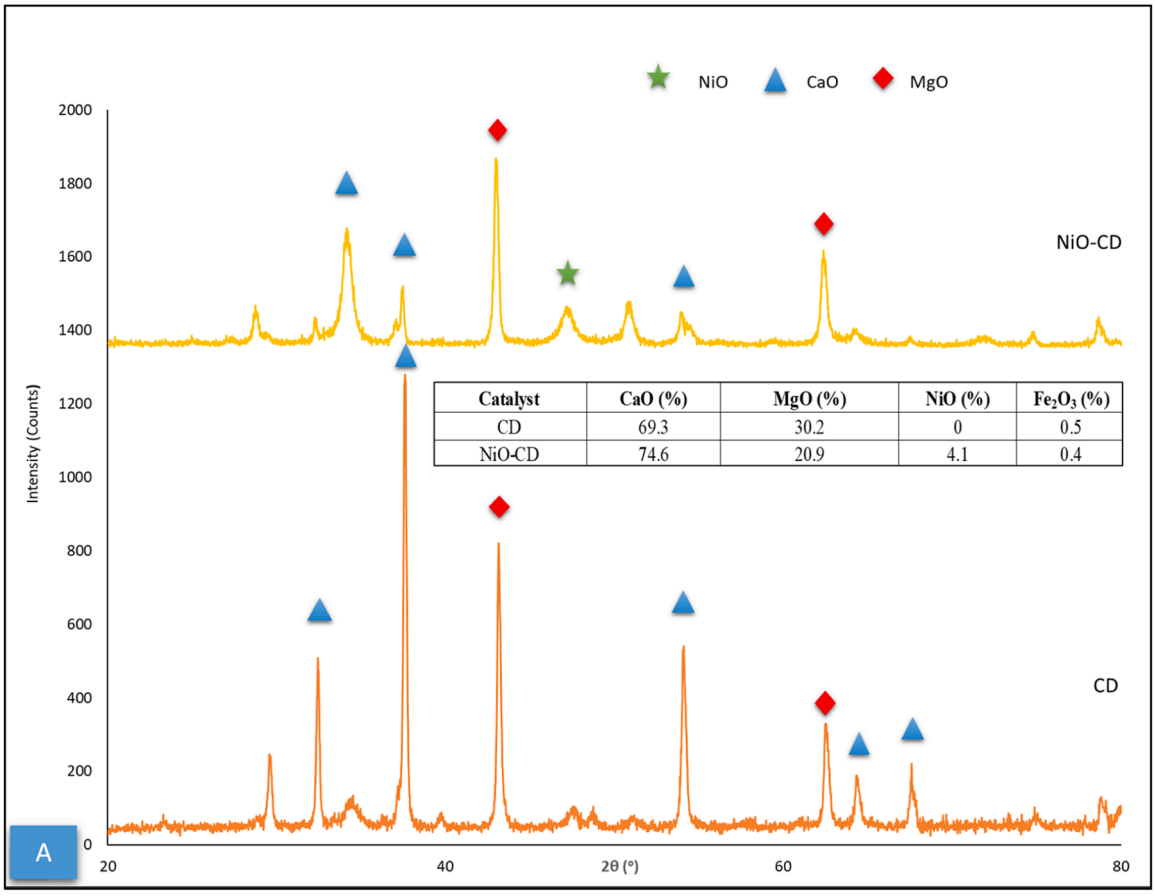

Catalyst	CaO (%)	MgO (%)	NiO (%)	Fe_2O_3 (%)
CD	69.3	30.2	0	0.5
NiO-CD	74.6	20.9	4.1	0.4

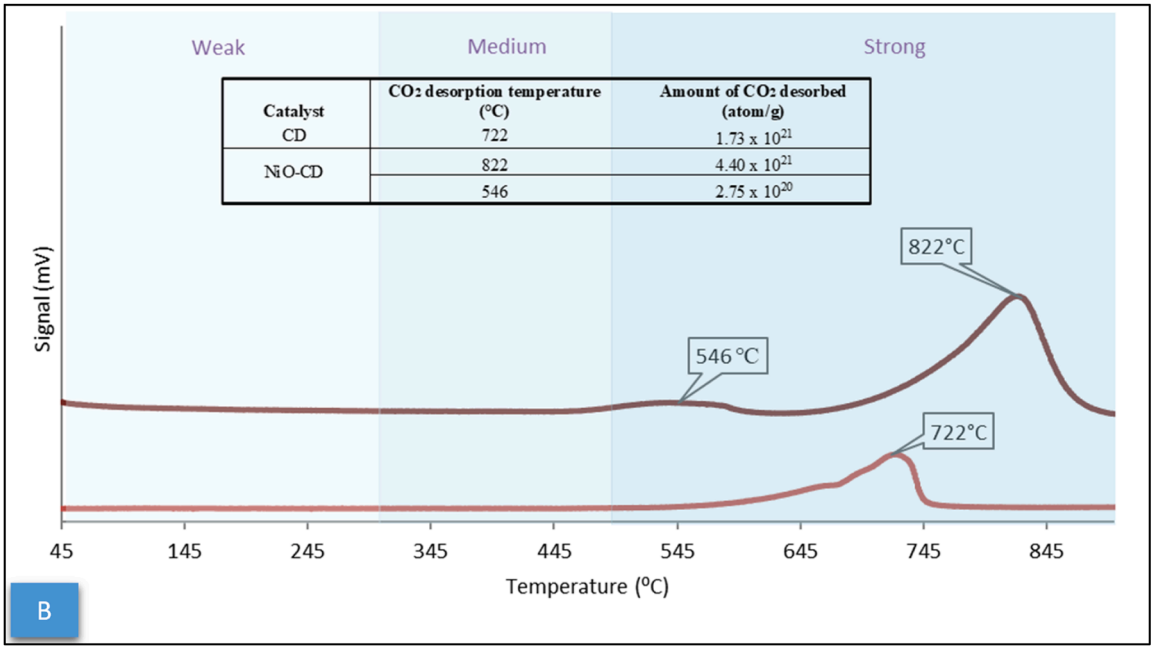

Catalyst	CO_2 desorption temperature (°C)	Amount of CO_2 desorbed (atom/g)
CD	722	1.73×10^{21}
NiO-CD	822	4.40×10^{21}
	546	2.75×10^{20}

Fig. 2. Physicochemical properties and morphology of the synthesized dolomite catalyst.

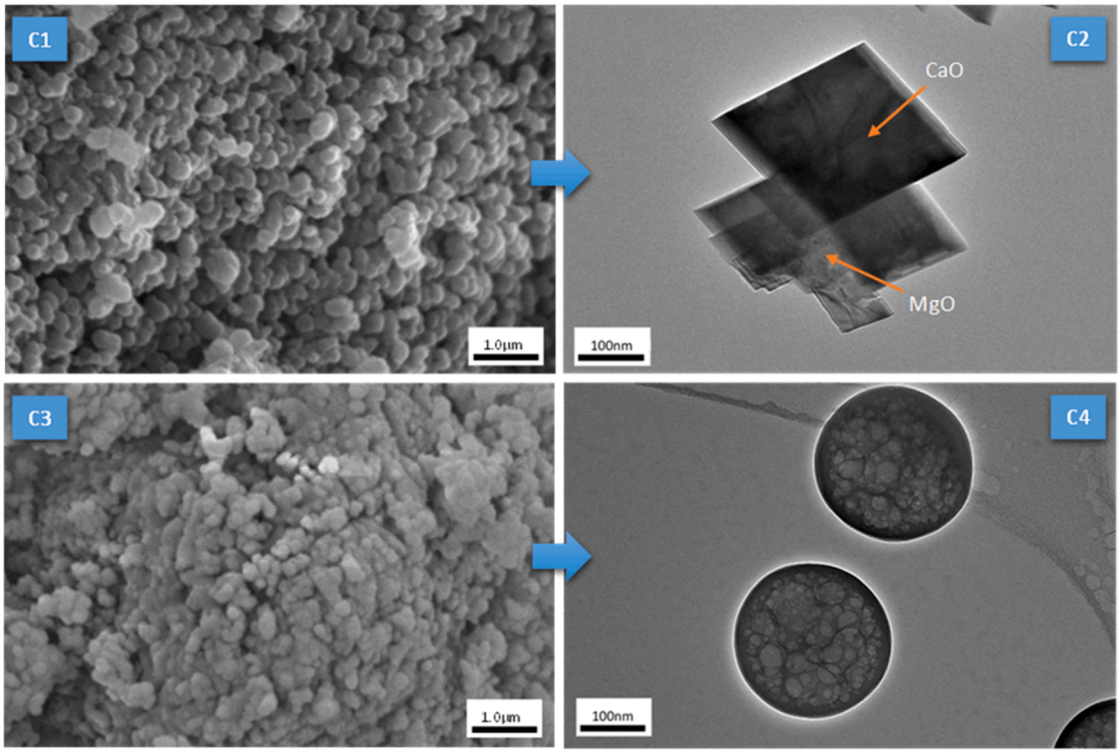

Catalyst	Surface Area (m^2/g)	Average pore diameter (nm)	Pore volume (cm^3/g)
CD	12	63.1	0.24
NiO-CD	18.2	48.2	0.22

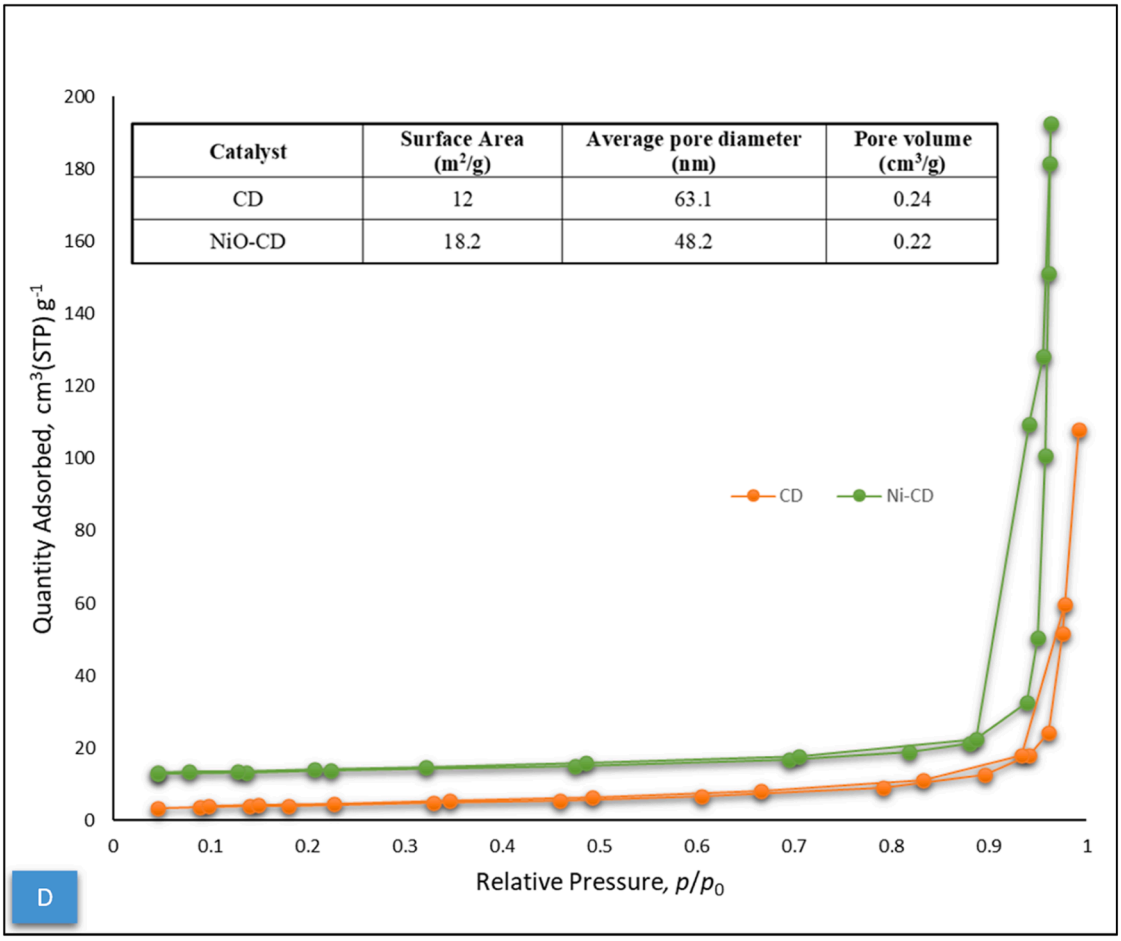

Fig. 2. (*continued*).

NiO—CaO phase with the unidentified poorly crystalline CaO-MgO phase.

The BET analysis on the synthesized catalysts is tabulated in Fig. 2 (D). The surface area of the CD and modified NiO—CD catalyst are 12.0 and 18.2 m^2/g, respectively. The result indicating the surface area increase suggests the successful doping of NiO particles on the CD catalyst. Adding NiO particles creates a more active site for chemical reactions and improves thermal stabilization. The pore volume data shows a slight decrease from 0.24 cm^3/g of synthesized CD catalyst to 0.22 cm^3/g of modified NiO—CD catalyst. This could be due to the aggregation of NiO particles, which causes a pore blockage effect on the support CD catalyst. The average pore diameter for the CD catalyst was 63.1 nm, while the nickel-modified catalyst exhibited a smaller pore diameter of 48.2 nm. The reduction in pore diameter could be attributed to pore constriction, which results from the doping of NiO particles. The data on the porosity suggest the improvement in the dolomite structure from a macroporous structure (pore diameter >50 nm) to a mesoporous structure (pore diameter between 2 and 50 nm). This structure improvement will provide additional deoxygenation pathways to yield more hydrocarbon compounds and reduce oxygenated compounds in green diesel.

Fig. 2(D) displays the N_2 adsorption-desorption isotherms of the synthesized CD and NiO—CD catalysts. The N_2 adsorption-desorption isotherms of the CD catalyst exhibited type III isotherms with type 3 hysteresis (H3). The macroporous adsorbent exhibited type III isotherms, indicating extremely weak interactions between the adsorbate and adsorbent. H3 hysteresis is observed in relation to the formation of slit-like pores by loose assemblages of platelike particles. Conversely, the NiO—CD catalyst exhibits type IV isotherms with type II hysteresis (H2), which is consistent with the IUPAC classification. Type IV isotherms indicate the presence of a mesoporous adsorbent, and the adsorption process on mesoporous substances involves the formation of several layers of adsorbate followed by capillary condensation. Toncón - Leal et al. [58] state that the scanning hysteresis loop offers insights on the relationship between the pore network, its connectivity, and the distribution of pore sizes in mesoporous materials. Within a relative pressure range of 0.84 to 1.00, the isotherms for both catalysts displayed the characteristic hysteresis loops commonly observed in mesoporous materials.

3.2. Effect of operating temperature

3.2.1. Product distribution using mass balance

The effect of catalytic deoxygenation (deCOx) of SO using the synthesized NiO—CD catalyst on the conversion is tabulated in Table 3.

The reactions were conducted at varied temperatures with constant catalyst loading (5 wt.%) for 30 min with a nitrogen gas flow rate of 150 cm^3/min. The conversions of SO (sum of liquid and estimation of gas produced) and product distribution were calculated based on weight percentage (wt.%). The findings indicate that the temperature of the deCOx reaction had a significant impact on conversion, with the highest conversion of 97.17% achieved at 450 °C operating temperature. The increase in temperature also has a significant impact on the formation of coke. These results show that catalytic deCOx favours high-temperature conditions to produce a high yield of green diesel and reduce the by-product formation such as coke. The finding is consistent with past studies conducted by Tamunaidu and Bhatia, [5] and Hafriz et al. [53]. The increasing of deCOx reaction temperature has a minor effect on the reduction of soap formation, but no substantial change in acid phase formation is seen. At higher temperatures, the thermal decomposition reactions of the SO become more extensive, leading to the formation of smaller and more volatile molecules. These smaller molecules can then condense into a liquid phase to form green diesel. Therefore, increasing deCOx temperature can promote green diesel formation and increase its yield with the additional function of base NiO—CD as a deCOx catalyst. Ranizang et al. [4] found that catalytic pyrolysis of fuel oil blended stock (FOBS) with metal oxide catalysts such as MgO, CaO, Na_2CO_3 and Fe_2O_3 produces a high yield of pyrolysis oil in the hydrocarbon range of C_{12}–C_{22}. The deactivation of the catalyst was due to the coke formation presence on the catalyst surface which is it can obstruct the active sites of the catalyst and prevent the reaction from taking place [59]. According to Shafihi et al. [60], in catalytic deoxygenation of waste cooking oil using $SO4^{2-}$-Fe_2O_3/Al_2O_3 catalyst, coke formation/carbon deposition occurs via two solid phase reactions: triglyceride condensation (Eq. (6)) or aromatic hydrocarbon polymerization (Eq. (7)).

Table 3
The product distribution of catalytic pyrolysis of SO using different operating temperatures (5 wt.% of NiO—CD catalyst, 150 cm^3/min of flow nitrogen gas, 30 min reaction time).

Product Distribution (wt.%)	350 °C	370 °C	380 °C	400 °C	420 °C	450 °C
Conversion of Soybean Oil, $\Sigma^{(a+b)}$	38.50	35.83	50.80	55.02	75.41	97.17
Liquid Product[a]	24.82	23.63	35.37	38.08	47.13	61.06
• **Green diesel**	22.48	21.06	33.07	36.24	44.86	58.70
• **acid phase**	1.32	1.36	1.45	1.03	1.47	1.58
• **soap**	1.02	1.21	0.85	0.81	0.80	0.78
Gas Product[b]	13.68	12.20	15.43	16.94	28.28	36.11
Coke	61.50	64.17	49.20	44.98	24.59	2.83

$$\text{Condensation}: \ \text{Triglyceride (WCO)} \rightarrow \text{Coke/Carbon}_{(s)} \tag{6}$$

$$\text{Polymerization}: \ C_n - H_n \ \text{(Aromatics)} \rightarrow \text{Coke/Carbon}_{(s)} \tag{7}$$

Fig. 3 depicts the green diesel produced at various operating temperatures. The green diesel appears to be darker at higher reaction temperatures, this is most likely due to thermal degradation products forming and could be due to high formation of ketones and aromatic compounds (green diesel at 450 °C). Therefore, controlling the catalytic deCOx conditions and feedstock quality is important for producing high-quality green diesel with desirable properties. As reported by Zikri et al. [61], more blackish colours and odours of liquid products have been produced at high reaction temperatures resulting in hydrocarbon formation from aromatic compounds and carbon deposits (coke).

3.2.2. Chemical composition of green diesel

Fig. 4 illustrates the effect of deCOx reaction temperature on hydrocarbon, oxygenated compound and oxygen removal percentages. There is a definite pattern of increasing hydrocarbon percentage as temperature increases from 370 °C to 420 °C, with a slight reduction at 450 °C.

A similar pattern is seen in oxygen removal percentage, with the highest percentage being 83.5% at 420 °C. In the study conducted by Asikin Mijan et al. [62] to maintain the quality of the final product of pyrolysis oil, the improvement of the deCOx pathway could be achieved due to the catalyst's performance and ability to efficiently remove oxygen content while minimising carbon loss. According to research conducted by Asikin Mijan et al. [62] and Hafriz et al. [63], it was concluded that dehydration (Eq. (8)) and cracking reaction (Eqs. (9) & (10)) facilitated due to acidic sites present during the catalysis process. In contrast, basic sites mostly promoted deCOx pathways (Eqs. (11) & (12)) while also partially eliminating oxygen from the triglyceride simultaneously.

Dehydration;

$$R - COOH \rightarrow RCO + H_2O \tag{8}$$

Decarboxylation;

$$R_x - COOH \rightarrow R_{x-1}H + R_xCOOH \tag{9}$$

$$R_x - R_y \rightarrow R_x = CH + R_y = CH \tag{10}$$

Decarboxylation;

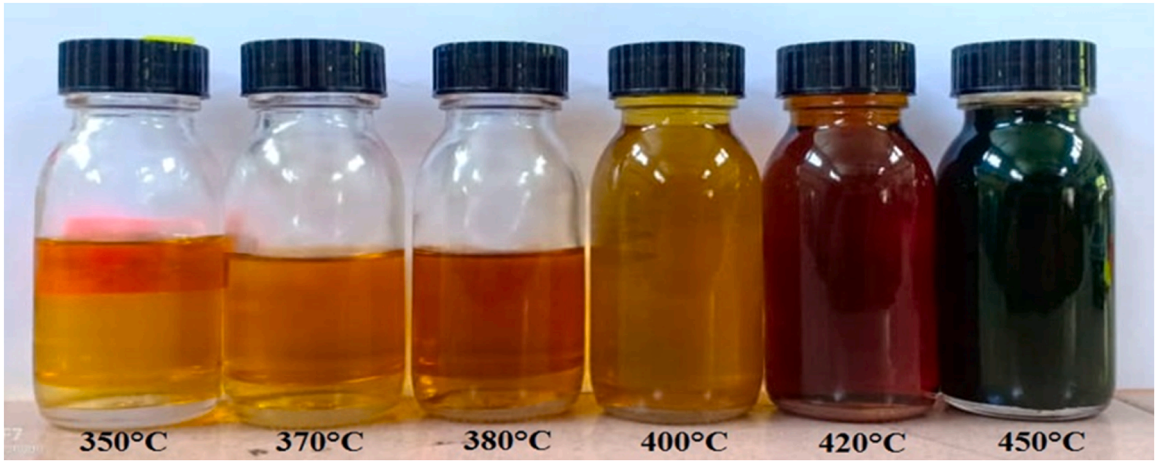

Fig. 3. Colour of produced green fuel at various operating temperatures.

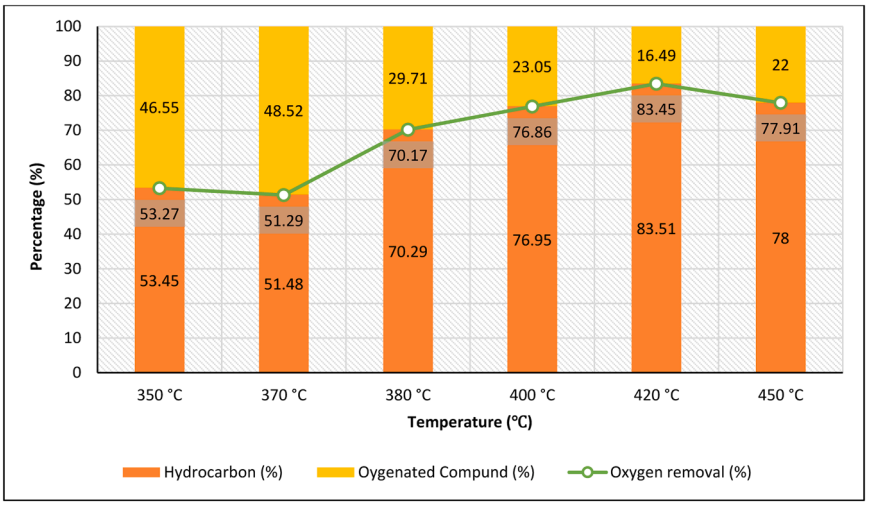

Fig. 4. The composition of green diesel under different temperatures applied.

Table 4
Composition profile of oxygenated compound in green diesel.

Product Distribution (%)	350 °C	370 °C	380 °C	400 °C	420 °C	450 °C
Total Oxygenated Product	46.55	48.52	29.71	23.05	16.49	22.00
• **Esters**	1.64	0.50	0.00	0.54	0.28	2.24
• **Carboxylic Acid**	31.51	35.24	17.08	11.11	4.64	0.42
• **Ketone**	1.12	1.42	2.62	5.12	4.84	13.32
• **Alcohol**	9.89	8.86	5.11	3.52	4.79	5.64
• **Others**	2.39	2.50	4.90	2.76	1.94	0.38

$$R - COOH \rightarrow C_n - H_{2n+2}(\text{Alkanes}) + CO_2 \quad (11)$$

Decarbonylation;

$$R - COOH \rightarrow C_n - H_{2n}\ (\text{Alkenes}) + CO + H_2O(\text{acid phase}) \quad (12)$$

As mentioned previously, a slightly lower percentage of hydrocarbon (78%) was found at a 450 °C reaction temperature compared to 420 °C. The increase in the percentage of oxygenated compounds was most likely due to the catalyst's decreased cracking activity. This finding was consistent with a recent work [53], which shows a decreased hydrocarbon oil yield with the oxygenated compound increase at a reaction temperature of 430 °C. In addition, at higher temperatures, the decomposition reactions of the organic compounds become more complex and can involve radical intermediates that react with oxygen present in the system. Specifically, at high temperatures, the oxygen-containing functional groups in soybean oil can undergo thermal decomposition, forming reactive intermediates such as carbonyl and carboxyl radicals. These radicals then can react with molecular oxygen present in the deoxygenation process system, forming additional oxygenated or undesirable compounds. According to prior research, the presence of oxygen in various aliphatic and aromatic oxygenates will affect the quality of the green diesel. In a study by Jenkins et al. [64], oxygenated compounds have a lower energy density than hydrocarbons, meaning they deliver less energy per unit of volume or mass. As a result, they are less efficient as fuels. Therefore, the total oxygenated compounds in green diesel must be reduced to improve their stability and reduce the risk of corrosion in fuel systems.

The composition of the oxygenated compound was further analysed and the profile is tabulated in Table 4. It is important to balance the presence of oxygenated compounds in green fuel and to carefully control the concentration of these compounds in order to optimize green fuel performance and minimize negative effects. Based on Table 4, increasing the deCOx reaction temperature can lead to decreased production of oxygenated compounds during green diesel production via catalytic deCOx of SO. However, at 450 °C, the amount of oxygenated compound was increased to 22.0%.

This might be due to the decomposition reactions of the organic compounds (in SO) at high temperatures becoming more complex and leading to the formation of reactive intermediates such as carbonyl and

carboxyl radicals. The involvement of these radical intermediates that react with oxygen molecules leads to the formation of additional oxygenated compounds present in the reaction system. A similar finding had been reported by Hafriz et al. [53] and Ali et al. [25]; the researchers found that the deoxygenation activity was retarded at high reaction temperatures due to the increment of the oxygenated compound at 430 °C and 450 °C, respectively. Table 4 shows that increasing the reaction temperature decreases the carboxylic acid and alcohol content in green diesel while marginally increasing ketone formation. This is most likely because higher temperatures promote more extensive cracking and isomerization of the hydrocarbon feedstocks, forming a wider range of molecular species, including ketones. High quantities of oxygenated compounds are undesirable since they result in high acid value, fuel corrosion, and an increase in cloud and pour points [25].

The composition of hydrocarbon observed in the green diesel at various deCOx reaction temperatures consists primarily of straight alkanes and alkenes, as presented in Table 7. Because hydrocarbons have a higher energy density than other molecules found in renewable diesel, such as oxygenates or nitrogen compounds, raising their concentration in green diesel can have various benefits. The increase in straight alkane formation occurred after the release of the CO_2 group from the soybean oil via decarboxylation reaction (Eq. (11)) and oligomerization of light alkenes during carboxylic acid deoxygenation (deCOx). Meanwhile, decarbonylation, as described in Eq. (12), was used to create alkenes by removing carbon monoxide, CO, and water, H_2O molecules. The increase in reaction temperature at optimum conditions will increase deCOx activity through the increase of alkanes and alkenes composition in green diesel. The temperature of the reaction also determines the reaction pathway assigned by the process selectivity [65–67].

The product selectivity based on the carbon number measured with GC–MS is shown in Fig. 5**(A)**. The green diesel contains a variety of carbon numbers ranging from C_8 to C_{18}, with a minimum number of hydrocarbons ranging from C_{19} to C_{24}. The majority of product yielded using NiO—CD catalyst was $C_{17}>C_{15}>C_{11}$ (350 and 370 °C), $C_{15}>C_{17}>C_{13}$ (380 and 400 °C), $C_{16}>C_{17}>C_9$ (420 °C) and $C_{16}>C_{17}>C_{13}$ (450 °C). The formation of hydrocarbon with low-range carbon numbers of C_{17} and C_{15} could be due to further secondary thermal cracking leading to a shorter chain of hydrocarbon after the deoxygenation reaction. Besides that, decomposition reactions of the organic compounds become more complex at high temperatures resulting in the high formation of C_{16} at temperatures of 420 °C and 450 °C. In high-temperature conditions, cracking and recombination reactions can occur simultaneously, resulting in a complex combination of products. The inclusion of a NiO—CD catalyst can additionally impact these processes by modifying the activation energy and selectivity of specific pathways. Besides that, temperature controls the breakdown process of the hydrocarbon molecules and alters the amount of product selectivity. In addition, the synthesized NiO—CD catalyst played an important role in manipulating the deCOx and cracking pathway. NiO—CD catalyst rendered mesoporous structure and synergistic effects of bi-functional NiO—CaO/MgO (acid-base) properties which are preferred by the deCOx pathway in the catalytic deCOx process.

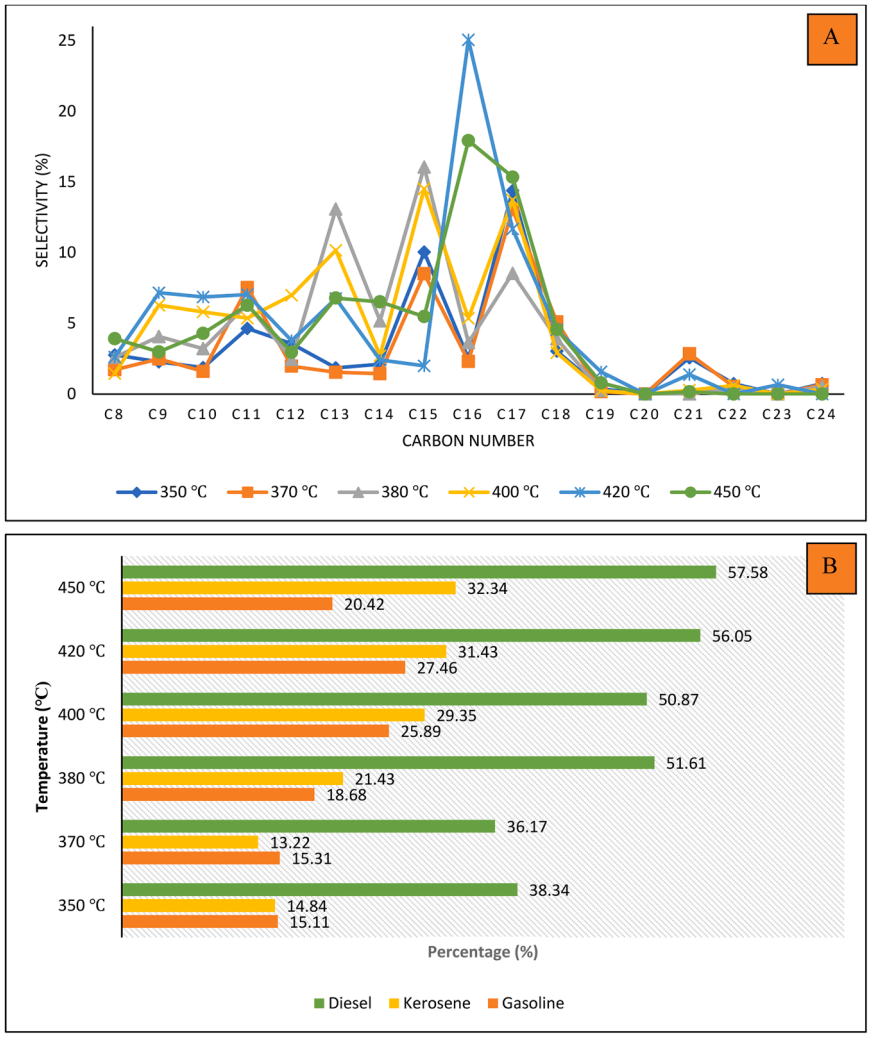

Fig. 5: A). Product selectivity based on carbon number and B) Classification of liquid product under different operating temperatures.

Table 5
The product distribution of catalytic pyrolysis of soybean oil at various nitrogen gas flows. (5 wt.% of NiO—CD catalyst, 420 °C reaction temperature & 30 min reaction time).

Nitrogen flowrate (cm^3/min)	50	150	250	350
Conversion of Soybean Oil, $^{\Sigma\,(a+b)}$	63.66	75.41	79.00	79.33
Liquid Product[a]	44.06	47.13	54.67	55.33
• **Green diesel**	41.80	44.86	51.93	52.00
• **acid phase**	1.31	1.47	1.36	1.76
• **soap**	0.95	0.80	1.38	1.57
Gas Product[b]	19.60	28.28	24.33	24.00
Coke	36.34	24.59	21.00	20.67

In Fig. 5(B) the liquid hydrocarbons are further classified into gasoline (C_8–C_{12}), diesel (C_8–C_{24}), and kerosene (alkanes, cycloalkanes, and aromatic compounds with C_8–C_{24} hydrocarbon numbers) range. It can be seen that the green diesel contains primarily diesel at all temperatures, with the maximum percentage recorded between 420 and 450 °C. At high deCOx reaction temperatures, aggressive C—C scission occurred more easily than C—O scission, non-volatile C_8–C_{12} light fractions were selectively produced and indicating that the NiO—CD catalyst catalyzed the simultaneous cracking- deCOx reaction. According to Pal et al. [3], due to the C—C bonds breaking and aromatic hydrocarbon formation, the lower temperature range will produce a long chain of hydrocarbon, whereas the higher temperature range will produce a short chain of carbon. It can be concluded that the best operating temperature for a deCOx reaction using a NiO—CD catalyst is 420 °C. This deCOx reaction temperature was selected based on the yield of green diesel (47.13 wt.%), hydrocarbon composition (83.51%), and the color of green diesel produced.

3.3. Effect of the flow of nitrogen gas

3.3.1. Product distribution using mass balance

The effect of different nitrogen gas flow rates on catalytic deCOx of a modified NiO—CD catalyst was investigated at a constant reaction temperature of 420 °C for 30 min. The calculated product distribution and conversions are presented in Table 5.

The results show increased conversion and yield of liquid products as the nitrogen flow increases. Nevertheless, raising the N_2 flow rate above 150 cm^3/min has negligible effects since the reactant's reaction time within the catalyst is limited due to a shortened residence time. In addition, a system may encounter a mass transfer constraint when the active sites become saturated and increasing the flow of N_2 does not result in a meaningful improvement in conversion. The highest conversion and yield of 79.3% and 52%, respectively, were observed when using a 350 cm^3/min flow of nitrogen. During the deCOx process, nitrogen gas will act as a carrier gas, assisting in maintaining a low-oxygen atmosphere and can condense any vapor quickly and easily. The increase in the nitrogen flow however increases the soap formation and acid phase too. The use of a base NiO—CD catalyst promotes the hydrolysis of the triglycerides into their component fatty acids and glycerol, which then react with the base catalyst to form soap [68]. The soap formation can be observed through the gas outlet at reaction temperatures of 200 – 250 °C could be due to the cooling effect of nitrogen gas. The hydrolysis of triglycerides requires the presence of water, which can be provided by the reaction itself (i.e., water (acid phase) is a by-product of the reaction) as mentioned in **Eq. 12**. The base catalyst or support catalyst, CaO/MgO provides the necessary alkaline conditions to promote the hydrolysis reaction and the subsequent saponification of the fatty acids. It is worth noting that soap formation is not always desired in the catalytic deCOx of triglycerides, as it can decrease the yield of green fuel products. Therefore, the modification of the catalyst and optimal reaction conditions must be carefully synthesized and optimized respectively, in order to maximize the yield of desired products and minimize other by-products such as soap formation, acid phase and coke. Coke formation can lead to the deactivation of the NiO—CD catalyst and reduce the efficiency of the process. According to Fig. 6, the oil produced was a dark brown colour, which might be attributed to the presence of aromatic and ketones, which are formed during the pyrolysis process. Based on Zhang et al. [69] and Lee et al. [70], the chemical composition of pyrolytic oils, which includes the presence of ketones and aromatic compounds, is determined by the nature of the feedstock and the specific conditions of the pyrolysis process, such as temperature and heating rate. Aside from the presence of these two compounds, other contaminants such as coke and water can contribute to the dark colour too. These contaminants can also have an effect on the green diesel properties such as stability, cetane number, and viscosity.

3.3.2. Chemical composition of green diesel

The green diesel was further evaluated for its composition and the results are shown in Fig. 7. The findings appear to contradict those on conversion and yield.

There is a decreasing trend of hydrocarbon percentage as the increasing of nitrogen flow rate in deCOx reaction. The finding suggests that the increasing nitrogen flow rate in catalytic deCOx could reduce the contact time between oil and the synthesized catalyst, which can affect the yield and selectivity of hydrocarbon produced. Despite the decreasing trend observed, the percentage of hydrocarbon remains higher than 80% for all flows. A higher oxygenated compound was observed at a higher flow rate. This is because the soybean oil was not totally cracked and catalyzed to produce more hydrocarbon compounds

Fig. 6. The green diesel generated at different flows of nitrogen gas.

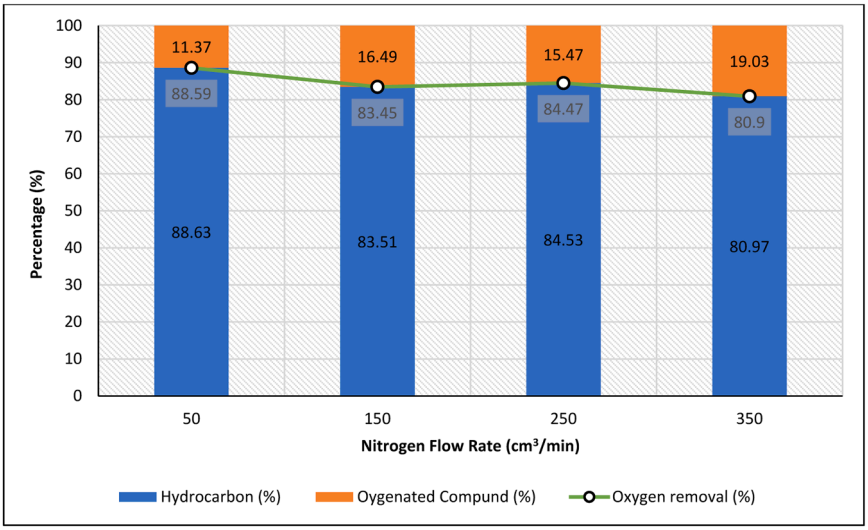

Fig. 7. The composition of green diesel under the different flows of nitrogen gas.

Table 6
Composition profile of oxygenated compound in green diesel.

Product Distribution (%)	50	150	250	350
Total Oxygenated Product	11.37	16.49	15.47	19.03
• **Esters**	0.23	0.28	0.66	0.48
• **Carboxylic Acid**	0.00	4.64	0.00	0.55
• **Ketone**	5.36	4.84	6.58	8.14
• **Alcohol**	3.53	4.79	7.96	8.46
• **Others**	2.25	1.94	0.27	1.40

due to the high purging of nitrogen gas in the deCOx reaction. In addition, a high flow rate of nitrogen gas can also reduce the contact time between the SO and NiO—CD catalyst, which can affect the selectivity of the liquid product and lead to changes in the chemical composition of the final product, green fuel. However, the hydrocarbon compound produced was >80% for a different flow rate of nitrogen gas set-up. The percentage of removal oxygenated compound was increased in the order of 50 cm^3/min > 250 cm^3/min > 150 cm^3/min > 350 cm^3/min. The result showed that under different nitrogen flow rates, they were capable of affecting the hydrocarbon yield and improving the performance of catalytic activity to remove the oxygenated compound of green fuel produced.

As tabulated in Table 6, the oxygenated compounds consist of esters, carboxylic acid, ketone, alcohol and other by-products. This is most likely due to nitrogen's cooling effect, which could lower the overall temperature of the reaction. As a result, there were fewer hydrocarbons and more oxygenated molecules formed. The high formation of ketone compound might be due to the high purging of nitrogen gas and the presence of base NiO—CD catalyst in catalytic deCOx of SO. Ketones can be intermediate compounds in the production of green fuel which can be produced during the first step of the process before going further converted into hydrocarbons through the use of in situ hydrogenation. Hydrogenation involves the addition of hydrogen to the ketones, which results in the formation of alcohols. The alcohols can then be dehydrated to form alkenes, which can be further hydrogenated to form the final diesel-like fuel. However, as reported by Chen *et al.* [71], the ketone compound is a compound that is directly produced from the ketonization of carboxylate species and gives rise to heavy products since the NiO–Fe_2O_3/MWCNT catalyst consists of strong basic sites. Based on Donnelly et al. [72], the presence of ketone compounds in biofuel has a positive effect on fuel properties. When biofuel consisting of 20% ketone compound was blended with jet A1, all fuel molecules produced suppressed the melting point below that of pure jet A-1. The amount of carboxylic acid produced was very low except at 150 cm^3/min of nitrogen gas flow. The carboxylic acid present will affect the acid value of the green fuel produced

A higher nitrogen flow rate can increase the velocity of the feedstock through the reactor, which can decrease the residence time and result in incomplete deCOx [73,74]. This effect has been observed clearly in decreasing hydrocarbon compounds with the increasing flow rate of Nitrogen gas, as summarised in Table 7. Based on Table 7, alkenes and alkanes compound with carbon number C_8–C_{24} were the most predominant with a concentration of 61–72%. The predominant alkenes compound in green fuel had shown that the decarbonylation reaction was the main promoting deCOx reaction pathway of SO using NiO—CD catalyst. However, it was contradicted as reported by Si et al. [75], who found that the basic sites play a major role in promoting decarboxylation reaction by retarding coke formation via a decrease in the deactivation rate of acidic catalysts.

The increasing formation of aromatic can be observed in Table 7. The formation of aromatic compounds can decrease the stability of green diesel by contributing to the formation of gums and other deposits, which can clog fuel filters and cause engine damage over time. Therefore, optimizing the nitrogen flow rate is an important factor in producing high-quality green diesel via deCOx. Nitrogen is often used during deCOx to create an inert atmosphere, which can help prevent unwanted side reactions and maintain the stability of the reaction environment. However, if the nitrogen flow rate is too high, it can reduce the concentration of in-situ hydrogen in the reactor, which may increase the aromatic compounds produced. The presence of in-situ hydrogen could contribute to the successful precipitation of Ni onto dolomite catalyst in catalytic deCOx reaction. A reduction of in-situ hydrogen concentration due to a high nitrogen flow rate could shift the reaction pathway towards the formation of aromatics. As reported by Huo et al. [76] and Collard et al. [77], nickel impregnation catalyzes

Table 7
Composition profile of hydrocarbon compound in green diesel.

Product Distribution (%)	50	150	250	350
Total Hydrocarbon Product	88.63	83.51	84.53	80.97
• **Alkane**	28.58	25.27	25.97	25.46
• **Cycloalkane**	5.49	3.57	4.94	4.68
• **Alkene**	42.77	43.41	43.94	35.96
• **Cycloalkene**	3.58	2.23	3.81	3.64
• **Diene**	0.86	3.55	1.26	3.49
• **Alkyne**	4.04	2.89	1.93	3.98
• **Aromatic**	3.31	2.59	2.68	3.76

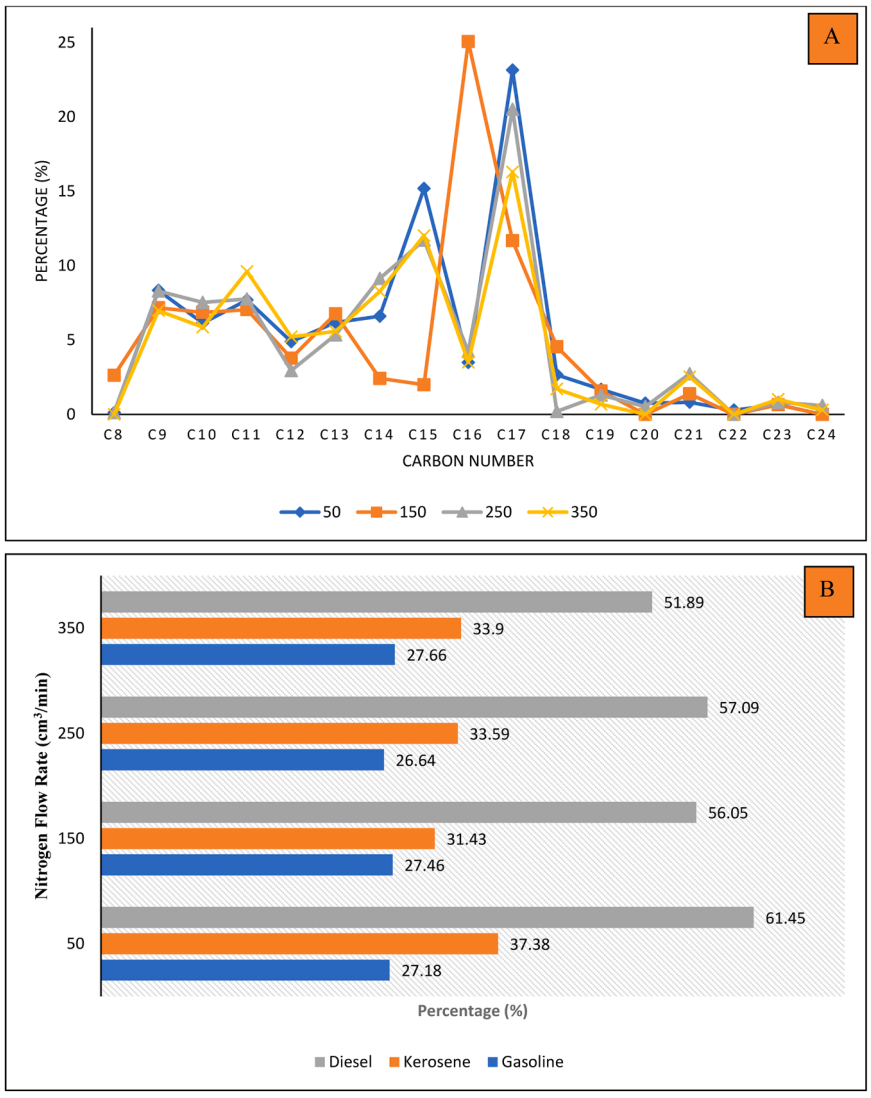

Fig. 8: A). Product selectivity based on carbon number and B) Classification of the liquid product under different nitrogen flow rates.

dehydration and decarboxylation reactions and promotes aromatic ring rearrangement, resulting in a high hydrogen yield. Besides that, the presence of nitrogen can also affect reaction kinetics, potentially resulting in changes in reaction product selectivity. Therefore, it is important to optimize the nitrogen flow rate during deCOx to balance the need for a stable reaction environment with the potential for unwanted side reactions.

The effect of nitrogen flow rate on product selectivity in the production of green diesel is largely dependent on the specific reaction conditions and catalyst used. In general, higher nitrogen flow rates tend to improve the selectivity and yield of green fuel by preventing coke formation and reducing the amount of undesirable by-products. However, excessively high nitrogen flow rates can also decrease the reaction rate and conversion efficiency, resulting in a decrease in hydrocarbon compounds as shown in Table 7. The decrease in hydrocarbon compound will affect the distribution of the desired product with a range of hydrocarbon carbon numbers C_8–C_{24}. The predominant hydrocarbon carbon number of the yielded product under different nitrogen gas flow rates shown in Fig. 8(A) was C_{17} and C_{15} due to decarbonylation and decarboxylation of C_{16} and C_{18} fatty acids. However, catalytic deCOx reaction under a nitrogen flow rate of 150 cm^3/min was predominantly by hydrocarbon with a carbon number of 16 (C_{16}) and this could be due to further C—C cracking of hydrocarbon, C_{17}. Besides that, the small content of the short chain of C_8–C_9 (6.97–9.79%) and a long chain of C_{19}–C_{24} (3.59–5.96%) has been observed in the deCOx profile as shown in Fig. 8(A). The short hydrocarbon of C_8–C_9 was possibly generated via auto-thermal cracking of C_{17} at high reaction temperatures, while the formation hydrocarbon of C_{19}–C_{24} was generated due to the secondary side reaction of the oligomerization reaction. Oligomerization reactions involve contacting the short-chain alkenes with a NiO—CD catalyst in order to produce a longer-chain molecule, C_{19}–C_{24} via the polymerization process.

In Fig. 8(B), the liquid hydrocarbons are further classified into gasoline, diesel, and kerosene-like fuel. It can be seen that green diesel contains primarily diesel at all temperatures, with the maximum percentage recorded at 50 cm^3/min of nitrogen flow. It can be observed that a low nitrogen flow rate will produce high diesel selectivity because of the increase in contact time between the SO feedstock and NiO—CD catalyst. Indeed, the excessive active site and mesoporous structure of the bi-functional acid-base catalyst, NiO—CD, particularly on the acidic site, will promote deoxygenated product cracking and yield a rich light fraction of gasoline. The flow rate of nitrogen gas has no significant effect on the gasoline and kerosene selectivity. The study on the production of SO-based green diesel via catalytic deCOx using NiO—CD catalyst at the different flows of nitrogen was successfully investigated. The best flow rate of nitrogen gas in catalytic deCOx of SO using NiO—CD catalyst is 50 cm^3/min. This flow rate was selected based on the high formation of hydrocarbon composition (88.63%) and also the

Table 8
The comparison based on previous research and various catalysts in catalytic deCOx of SO under an oxygen-free environment.

No.	Feedstock	Catalyst	Condition (Catalyst loading/ Temp/ time/ N_2 flow rate)	Reactor type	Green diesel (wt.%)	HCs* yield (%)	Green Diesel selectivity (%)	References
1.	Soybean Oil	CaO	10 wt.% / 450 °C / - / 1.45 ml/ min	continuous fixed bed reactor	76.0	48.30	40.10	[78]
2.	Soybean Oil	Ni-Al-MCM-41	1–3 wt.% / 450 °C / 4 h / -	Tabular reactor	57.9	82.50	48.80	[79]
3.	Crude Soybean Oil	ZSM-5	0.003 wt.% / 450 °C / 45 min/ 42 ml/min	Micro fixed-bed reactor	–	27.83	1.03	[80]
4.	Soybean Oil	NiO—CD	5 wt.% / 420 °C / 30 min/ 50 cm^3/min	Distillation flask reactor	41.8	88.63	61.45	Present study

* HCs - Hydrocarbon.

high yield of green diesel products produced (41.80 wt.%).

3.3.3. Comparison of previous studies

Table 8 compares the studies on previous research and different catalysts in catalytic deCOx of soybean oil under purging of N_2 or oxygen-free environment. The catalyst presence and reaction parameters are affecting the yield and selectivity of hydrocarbon. As reported by GaO et al. [78], the maximum liquid condensate yield (76.0%) was obtained using a CaO catalyst at a pyrolysis temperature of 450 °C and 0.62 g min^{-1} feeding rate. The catalytic activity of this catalyst presents a good catalytic result over the zeolite catalyst used. Besides that, they found that the yield of liquid decreased with the increase of reaction temperature > 450 °C because of more violent reactions and the formation of secondary reactions. In the secondary reaction, the pyrolysis of soybean oil at a higher temperature was converted into a gas product and the enhancement of polymerization would reduce the yield of liquid fraction. The addition of CaO catalyst resulted in a significant change in product distribution, with selectivity towards high diesel-like fuel. Yu et al. [79] also demonstrated the best temperature reaction of catalytic deCOx under the flow of nitrogen gas at 450 °C. They discovered that Ni-Al-MCM-41 had the highest catalyst activity and good performance, yielding 57.9 wt.% of SO-based biofuel with 48.8% selectivity towards green diesel. The biofuel produced via catalytic pyrolysis with Ni-Al-MCM-41 catalyst was tested using China national (GB) standard methods, and the results showed that the biofuel produced has a good chance of serving as an alternative to traditional petroleum fuel. As mentioned by Emori et al. [80], the influence of gas purging was responsible for the increase of liquid compound yield and heavier hydrocarbon formation in the catalytic pyrolysis of SO using a ZSM-5 catalyst. The N_2 flow produces more H_2 gas in the production stream. However, they found out that, the selectivity towards green diesel is lower as compared to other studies stated in Table 8. As compared to the previous study under the purging of Nitrogen gas, the catalytic deoxygenation of SO using a synthesized NiO—CD catalyst resulted in a lower green diesel yield. However, when compared to different types of catalysts used, the hydrocarbon yield and selectivity towards green diesel were the highest. Therefore, the study on optimal conditions such as temperature reaction and flow rate of gas using certain catalysts via catalytic deCOx reaction should be conducted to produce a high yield of SO-based green diesel and hydrocarbon.

3.3.4. Proposed reaction mechanisms of catalytic deCOx of soybean oil

Fig. 9 illustrates the proposed mechanism in catalytic deCOx of SO using NiO—CD catalyst. The proposed reaction pathway was established based on the identified fatty acid composition of the reactant and the hydrocarbon composition of the SO-based green diesel produced from the deCOx reaction via GC–MS analysis results. Table 1 shows that SO contains 40.1% oleic acid, 29.4% palmitic acid and 14.1% stearic acid which accounts for most of the fatty acids contained in the feedstock. This feedstock composition produced green diesel with a high percentage of C_{15} and C_{17} hydrocarbons as observed in Figs. 5 and 8. This finding indicates that catalytic deCOx of SO with the presence of a synthesized NiO—CD catalyst promotes the formation of hydrocarbon derivatives in C_{15} and C_{17}. As stated in Fig. 9, pathway **1** shows that oleic

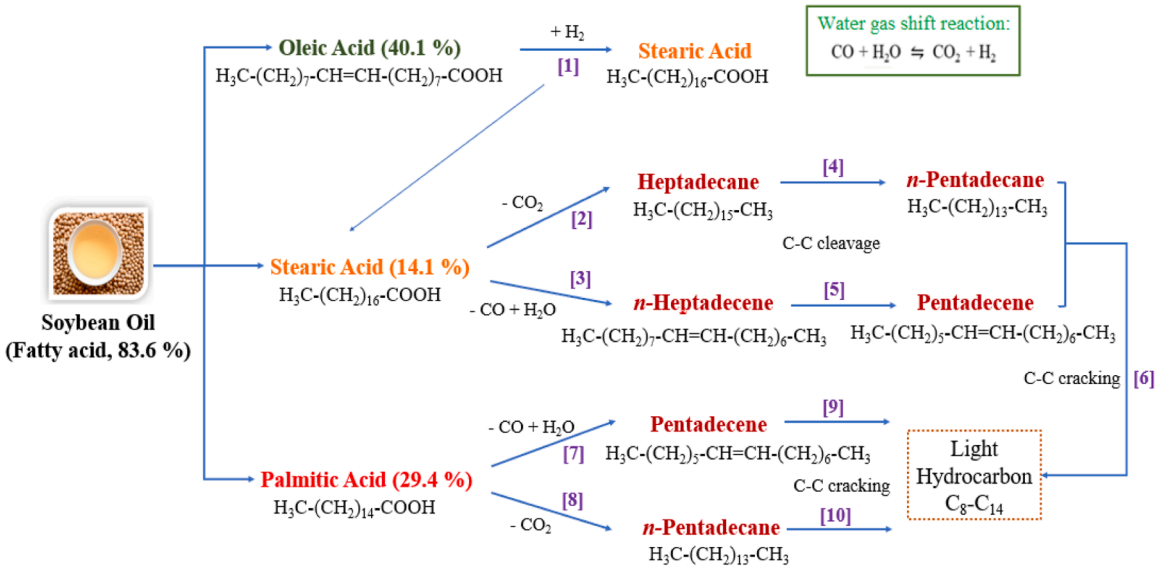

Fig. 9. The proposed catalytic deoxygenation reaction mechanism of Soybean Oil using a synthesized NiO—CD catalyst.

acid undergoes hydrogenation to produce steric acid as an intermediate product. The rich in-situ hydrogen is generated during the reaction via water gas shift (WGS), which promotes the breaking of oleic acid double bonds. Furthermore, the NiO—CD catalyst present will enhance the hydrogenation reaction by promoting the cleavage of carbon-oxygen bonds, which results in oxygen atoms removal from the SO molecules. The intermediate steric acid will be produced along with the existing steric acid in the feedstock and will be subjected to a deCOx reaction initiated by NiO and CaO active sites on the dolomite catalyst support. DeCOx reaction would remove CO_2, CO and H_2O from the stearic acid carbon chain through decarboxylation and decarbonylation (deCOx) reaction as suggested in pathways **2** and **3,** resulting in the production of heptadecane (C_{17}) and *n*-heptadecene (*n*-C_{17}). Further series of C—C bond cleavage mild cracking of heptadecane and *n*-hepatdecene would produce pentadecane, n-pentadecene and lighter hydrocarbon of C_8–C_{14} as shown in pathways **4, 5** and **6**. This was in line with the investigation done by Smoljan et al. [81] and Septriana et al. [82] on catalytic deCOx of fatty acids using NiO catalyst. A similar decarbonylation pathway would occur in palmitic acid to generate pentadecane from the releasing of CO and H_2O in pathway **7** while pathway **8** conveys the decarbolxylation route of palmitic acid to produce n-pentadecene. Further C—C cracking reaction of these C_{15} hydrocarbons at a mild condition would produce lighter hydrocarbon with a C_8–C_{14} carbon range as illustrated in pathways **9** and **10**. It can be concluded that these **1–10** pathways proposed for the catalytic deCOx of SO using the synthesized NiO—CD catalyst favors the decarboxylation and decarbonylation reactions due to the composition starting materials of the feedstock and the green diesel produced in Table 1, 5 and 7.

3.3.5. Life cycle cost analysis (LCCA) of stepwise green diesel (GD) production

Table 9 presents a comparison of the life cycle cost analysis (LCCA) for stepwise Green Diesel (GD) production. This LCC analysis examines the cost of the catalyst employed in the catalytic deoxygenation of soybean oil (SO) to produce GD. The catalysts utilized in this comparison consist of commercial zeolite and NiO—CD catalysts. The cost of the catalyst has been determined for 10 cycles of reusability for commercial zeolite (RM 213.40/kg) and 5 cycles for NiO—CD (RM 6.80/kg). The incremental participation in different phases of the biofuel production process has been taken into account when calculating the LCCA. The estimate was derived from the expenses incurred in manufacturing 100 kg of GD, which includes the net cost of materials, the associated production processes, and the overhead cost, with an additional 10% of the net cost. It also takes into account the cost of producing 1 kg of GD. Table 9 demonstrates that the feedstock cost accounted for the highest proportion, around 74.8%, of the overall cost of GD production using NiO—CD catalyst as compared to commercial zeolite catalyst (30.2%). Ong et al. [83] also discovered that the cost of the feedstock, crude palm oil (CPO), makes up 79% of the entire production cost of biodiesel. The feedstock quantity varied between these two catalyst types used as a result of the conversion efficiency of soybean oil (SO) into a 100 kg GD product. The cost of the catalyst was determined by the optimal catalyst loading conditions, which was 5% for the catalytic deoxygenation reaction. When comparing the costs of feedstock and material for different catalysts used, there is no substantial difference in cost. However, the introduction of a different catalyst in the catalytic deoxygenation process would lead to a wider cost differential, as shown in Table 9. It demonstrates how the cost of producing GD will depend on the catalyst's pricing. It is feasible to determine the cost of making 1 kg of GD using various catalyst types by performing a step-by-step examination of GD production. The LCC analysis can estimate the cost of GD at RM 10.42/kg using NiO—CD catalyst and RM 23.12/kg using commercial zeolite catalysts, depending on the type of catalyst used. Furthermore, it also does not take into account any taxes or government-imposed green electricity tariffs in Malaysia.

Table 9
Comparison of LCCA of GD production using a heterogeneous catalyst, NiO—CD and commercial zeolite catalyst.

No.	Stepwise Biofuel Production	Green Diesel Production using Commercial Zeolite	Green Diesel Production using NiO—CD
1.	Cost of Soybean Oil (SO) for production of 100 kg GD (amount × SO cost per kg)	117.65 kg x RM 5.40/ kg = RM 635.31 (85% conversion to 100 kg of GD) **Total: RM 635.31**	142.86 kg x RM 5.40/ kg = RM 771.44 (70% conversion to 100 kg of GD) **Total: RM 771.44**
2.	The catalyst amount estimated for the production of 100 kg of GD	5 wt.% of catalyst was used = 5.88 kg The cost of the catalyst used = 5.88 kg x RM 213.40 = RM 1254.79 **Total: RM 1254.79**	5 wt.% of catalyst was used = 7.143 kg The cost of the catalyst used = 7.143 kg x RM 6.80 = RM 48.57 **Total: RM 48.57**
3.	Industrial Nitrogen gas	Cost of industrial nitrogen gas = RM 4200.00/ 20 cycle = RM 210.00 **Total: RM 210.00**	Cost of industrial nitrogen gas = RM 4200.00/ 20 cycle = RM 210.00 **Total: RM 210.00**
4.	Cost of deoxygenation process involved in GD production	Utilities: Electricity 1 h x 7 kW x RM 0.1979* = RM 1.39 Utilities: Water (6 h) 0.1 m^3 x RM 2.07**= RM 0.207 **Total: RM 1.39 + RM 0.27 = RM 1.66**	Utilities: Electricity 1 h x 7 kW x RM 0.1979* = RM 1.39 Utilities: Water (6 h) 0.1 m^3 x RM 2.07**= RM 0.207 **Total: RM 1.39 + RM 0.27 = RM 1.66**
5.	Net cost (Cost of SO + Cost of catalyst + Cost of materials used + Cost of process involved in GD production)	RM 635.31 + RM 1254.79 + RM 210 + RM 1.66 = **RM 2101.76**	RM 771.44 + RM 48.57 + RM 210.00 + RM 1.66 = **RM 1031.67**
6.	Overhead cost (10% of net cost)	**RM 210.18**	**RM 10.32**
7.	The cost of producing 100 kg of GD	RM 2101.76 + RM 210.18 = **RM 2311.94**	RM 1031.67 + RM 10.32 = **RM 1041.99**
8.	The cost of producing 1 kg of GD	RM 2311.94 / 100 = **RM 23.12**	RM 1347.70 / 100 = **RM 10.42**

* Electricity tariff provided by Tenaga Nasional Berhad (TNB) Malaysia excluded green electricity tariff by GOV Malaysia.

** Water tariff for Higher Learning Institutions (HLIs) provided by Air Selangor (State GOV of Selangor, Malaysia).

4. Conclusion

The catalytic deCOx of SO into green diesel has been successfully generated using a low-cost NiO—CD catalyst. The dispersion of nickel metal onto calcined dolomite catalyst not only provides a more active site to catalyze the reactant particles of SO but also improves their thermal stability and textural mesoporosity of the synthesized NiO—CD catalyst. In addition, the presence of NiO species promotes the formation of acidic sites on the surface dolomite support catalyst system, resulting in a synergistic effect of bi-functional acid-base properties of the synthesized NiO—CD catalyst. The one-factor-at-a-time (OFAT) method was used to investigate the effect of reaction temperature and nitrogen gas flow rate on the catalytic deCOx of SO using a synthesized NiO—CD catalyst. A series of experiments found that temperature and nitrogen flow rate had a significant impact on green diesel yield, hydrocarbon percentage, and chemical composition. The best operating temperature via deCOx reaction of SO using NiO—CD catalyst was 420 °C with the highest yield of green diesel produced (47.13 wt.%) with the highest hydrocarbon composition (83.51%). Meanwhile, the best flow rate of nitrogen gas used was 50 cm^3/min. This flow rate was selected based on the high yield of green diesel produced (41.80 wt.%) with 88.63% hydrocarbon composition at reaction temperature of 420 °C for 30 min of reaction time. Therefore, it is important to optimize the reaction temperature and flow rate of nitrogen during the deCOx process using a

catalyst to balance the need for a stable reaction environment without the presence of potential unwanted side reactions. The modified Malaysia dolomite, NiO—CD catalyst has the potential to reduce the overall cost of green diesel production as compared to commercial zeolite catalyst through LCC analysis of stepwise of catalyst preparation and green diesel production.

CRediT authorship contribution statement

R.S.R.M. Hafriz: Writing – original draft, Validation, Software, Methodology, Investigation, Formal analysis, Data curation, Conceptualization. **S.H. Habib:** Writing – review & editing, Validation, Investigation, Data curation, Conceptualization. **N.A. Raof:** Writing – review & editing, Validation, Investigation, Conceptualization. **S.Z. Razali:** Validation, Investigation, Conceptualization. **R. Yunus:** Validation, Supervision, Resources, Project administration. **N.M. Razali:** Resources, Project administration. **A. Salmiaton:** Writing – review & editing, Validation, Supervision, Resources, Project administration, Methodology, Funding acquisition, Conceptualization.

Declaration of competing interest

The authors declare that they have no known competing financial interests or personal relationships that could have appeared to influence the work reported in this paper.

Acknowledgements

The authors acknowledge the financial support from the Ministry of Higher Education of Malaysia for the Fundamental Research Grant Scheme (FRGS/1/2020/TK0/UPM/02/15), the AAIBE Chair of Renewable Energy Grant No 201801KETTHA, 202201KETTHA and 202302KETTHA, BOLD Refresh Postdoctoral Fellowships (J510050002–1C-6) for funding this research publication.

References

[1] García-Moreno S, López-Ruiz VR. A review of the energy sector as a key factor in industry 4.0: the case of Spain. Energies (Basel) 2023:16. https://doi.org/10.3390/en16114446.
[2] Chua JY, Pen KM, Poi JV, Ooi KM, Yee KF. Upcycling of biomass waste from durian industry for green and sustainable applications: an analysis review in the Malaysia context. Energy Nexus 2023;10. https://doi.org/10.1016/j.nexus.2023.100203.
[3] Pal S, Kumar A, Sharma AK, Ghodke PK, Pandey S, Patel A. Recent advances in catalytic pyrolysis of municipal plastic waste for the production of hydrocarbon fuels. Processes 2022;10. https://doi.org/10.3390/pr10081497.
[4] Ranizang WNAAW, Yussuf MAM, Mohamed M, Jusoh M, Zakaria ZY. Catalytic pyrolysis of fuel oil blended stock for bio-oil production: a review. Chem Eng Trans 2022;97:373–8. https://doi.org/10.3303/CET2297063.
[5] Tamunaidu P, Bhatia S. Catalytic cracking of palm oil for the production of biofuels: optimization studies. Bioresour Technol 2007;98:3593–601. https://doi.org/10.1016/j.biortech.2006.11.028.
[6] Athar M, Zaidi S. A review of the feedstocks, catalysts, and intensification techniques for sustainable biodiesel production. J Environ Chem Eng 2020;8. https://doi.org/10.1016/j.jece.2020.104523.
[7] Kuan C, Neng M, Chan Y-B, Sim Y-L, Strothers J, Pratt L. Thermal transformation of palm waste to high-quality hydrocarbon fuel. Fuels 2020;1:2–14. https://doi.org/10.3390/fuels1010002.
[8] Haryani N, Taslim Irvan, Manurung R, Tambun R. Synthesis, Characterization, and Application of ZnO/ZSM-5 as Catalyst in The Cracking Process of Palm Methyl Esters. J Appl Eng Sci 2022;20:63–70. https://doi.org/10.5937/jaes0-31312.
[9] Neonufa G, Pratiwi M, Prakoso T, Purwadi R, Soerawidjaja T. Catalytic thermal decarboxylation of palm kernel oil basic soap into drop-in fuel. MATEC Web Conf 2019;268:06014. https://doi.org/10.1051/matecconf/201926806014.
[10] Altalhi AA, Mohamed EA, Morsy SM, Abou Kana MTH, Negm NA. Catalytic manufacture and characteristic valuation of biodiesel-biojet achieved from Jatropha curcas and waste cooking oils over chemically modified montmorillonite clay. J Mol Liq 2021;340. https://doi.org/10.1016/j.molliq.2021.117175.
[11] Scaldaferri CA, Pasa VMD. Production of jet fuel and green diesel range biohydrocarbons by hydroprocessing of soybean oil over niobium phosphate catalyst. Fuel 2019;245:458–66. https://doi.org/10.1016/j.fuel.2019.01.179.
[12] Naji SZ, Tye CT, Abd AA. State of the art of vegetable oil transformation into biofuels using catalytic cracking technology: recent trends and future perspectives. Process Biochem 2021;109:148–68. https://doi.org/10.1016/j.procbio.2021.06.020.
[13] Hansen S, Mirkouei A, Diaz LA. A comprehensive state-of-technology review for upgrading bio-oil to renewable or blended hydrocarbon fuels. Renewable Sustainable Energy Rev 2020;118. https://doi.org/10.1016/j.rser.2019.109548.
[14] da Costa AAF, de O. Pires LH, Padrón DR, Balu AM, da Rocha Filho GN, Luque R, do Nascimento LAS. Recent advances on catalytic deoxygenation of residues for bio-oil production: an overview. Mol Catal 2022;518. https://doi.org/10.1016/j.mcat.2021.112052.
[15] Veriansyah B, Han JY, Kim SK, Hong SA, Kim YJ, Lim JS, Shu YW, Oh SG, Kim J. Production of renewable diesel by hydroprocessing of soybean oil: effect of catalysts. Fuel 2012;94:578–85. https://doi.org/10.1016/j.fuel.2011.10.057.
[16] Cheah KW, Yusup S, Loy ACM, How BS, Skoulou V, Taylor MJ. Recent advances in the catalytic deoxygenation of plant oils and prototypical fatty acid models compounds: catalysis, process, and kinetics. Mol Catal 2022:523. https://doi.org/10.1016/j.mcat.2021.111469.
[17] Yıldız A, Goldfarb JL, Ceylan S. Sustainable hydrocarbon fuels via “one-pot” catalytic deoxygenation of waste cooking oil using inexpensive, unsupported metal oxide catalysts. Fuel 2020;263. https://doi.org/10.1016/j.fuel.2019.116750.
[18] Kumar R, Strezov V, Lovell E, Kan T, Weldekidan H, He J, Jahan S, Dastjerdi B, Scott J. Enhanced bio-oil deoxygenation activity by Cu/zeolite and Ni/zeolite catalysts in combined in-situ and ex-situ biomass pyrolysis. J Anal Appl Pyrolysis 2019;140:148–60. https://doi.org/10.1016/j.jaap.2019.03.008.
[19] Ooi XY, Gao W, Ong HC, Lee HV, Juan JC, Chen WH, Lee KT. Overview on catalytic deoxygenation for biofuel synthesis using metal oxide supported catalysts. Renewable Sustainable Energy Rev 2019;112:834–52. https://doi.org/10.1016/j.rser.2019.06.031.
[20] Rozmysłowicz B, Mäki-Arvela P, Tokarev A, Leino AR, Eränen K, Murzin DY. Influence of hydrogen in catalytic deoxygenation of fatty acids and their derivatives over Pd/C. Ind Eng Chem Res 2012:8922–7. https://doi.org/10.1021/ie202421x.
[21] Eschenbacher A, Jensen PA, Henriksen UB, Ahrenfeldt J, Ndoni S, Li C, Duus JØ, Mentzel UV, Jensen AD. Catalytic deoxygenation of vapors obtained from ablative fast pyrolysis of wheat straw using mesoporous HZSM-5. Fuel Process Technol 2019;194. https://doi.org/10.1016/j.fuproc.2019.106119.
[22] Khalit WNAW, Asikin-Mijan N, Marliza TS, Gamal MS, Shamsuddin MR, Saiman MI, Taufiq-Yap YH. Catalytic deoxygenation of waste cooking oil utilizing nickel oxide catalysts over various supports to produce renewable diesel fuel. Biomass Bioenergy 2021;154. https://doi.org/10.1016/j.biombioe.2021.106248.
[23] Morgan T, Santillan-Jimenez E, Harman-Ware AE, Ji Y, Grubb D, Crocker M. Catalytic deoxygenation of triglycerides to hydrocarbons over supported nickel catalysts. Chem Eng J 2012;189–190:346–55. https://doi.org/10.1016/j.cej.2012.02.027.
[24] Papageridis KN, Charisiou ND, Douvartzides S, Sebastian V, Hinder SJ, Baker MA, AlKhoori S, Polychronopoulou K, Goula MA. Promoting effect of CaO-MgO mixed oxide on Ni/γ-Al2O3 catalyst for selective catalytic deoxygenation of palm oil. Renew Energy 2020;162:1793–810. https://doi.org/10.1016/j.renene.2020.09.133.
[25] Ali SH, Hafriz RSRM, Shamsuddin AH, Salmiaton A. Production of liquid biofuel from sludge palm oil (SPO) using heterogeneous catalytic pyrolysis. J Appl Sci Eng (Taiwan) 2023;26:529–38. https://doi.org/10.6180/jase.202304_26(4).0009.
[26] Buyang Y, Nugraha RE, Holilah H, Bahruji H, Suprapto S, Jalil AA, Muryani M, Prasetyoko D. Dolomite catalyst for fast pyrolysis of waste cooking oil into hydrocarbon fuel. S Afr J Chem Eng 2023;45:60–72. https://doi.org/10.1016/j.sajce.2023.04.007.
[27] Xiao L, Li C, Chai D, Chen Y, Wang Z, Xu X, Wang Y, Geng Y, Dong L. Volatile compound profiling from soybean oil in the heating process. Food Sci Nutr 2020;8:1139–49. https://doi.org/10.1002/fsn3.1401.
[28] Fan X. Furan formation from fatty acids as a result of storage, gamma irradiation, UV-C and heat treatments. Food Chem 2015;175:439–44. https://doi.org/10.1016/j.foodchem.2014.12.002.
[29] Silva LMCE, de Melo MLP, Reis FVF, Monteiro MC, Dos Santos SM, Gomes BAQ, da Silva LHM. Comparison of the effects of Brazil nut oil and soybean oil on the cardiometabolic parameters of patients with metabolic syndrome: a randomized trial. Nutrients 2020;12. https://doi.org/10.3390/nu12010046.
[30] Souza LA, Silva FC, Maria ACL, Belem AL, Cecchin D, Barros MM. Response surface for biodiesel production from soybean oil by ethylic route. Agronomy Res 2020;18:1498–515. https://doi.org/10.15159/AR.20.065.
[31] Doná G, Cardozo-Filho L, Silva C, Castilhos F. Biodiesel production using supercritical methyl acetate in a tubular packed bed reactor. Fuel Process Technol 2013;106:605–10. https://doi.org/10.1016/j.fuproc.2012.09.047.
[32] Ruatpuia JVL, Halder G, Mohan S, Gurunathan B, Li H, Chai F, Basumatary S, Rokhum SLalthazuala. Microwave-assisted biodiesel production using ZIF-8 MOF-derived nanocatalyst: a process optimization, kinetics, thermodynamics and life cycle cost analysis. Energy Convers Manag 2023;292. https://doi.org/10.1016/j.enconman.2023.117418.
[33] Hafriz RSRM, Shafizah IN, Arifin NA, Salmiaton A, Yunus R, Yap YHT, Shamsuddin AH. Effect of Ni/Malaysian dolomite catalyst synthesis technique on deoxygenation reaction activity of waste cooking oil. Renew Energy 2021;178:128–43. https://doi.org/10.1016/j.renene.2021.06.074.
[34] Asikin-Mijan N, Lee HV, Abdulkareem-Alsultan G, Afandi A, Taufiq-Yap YH. Production of green diesel via cleaner catalytic deoxygenation of Jatropha curcas oil. J Clean Prod 2017;167:1048–59. https://doi.org/10.1016/j.jclepro.2016.10.023.
[35] Alsultan GA, Asikin-Mijan N, Lee HV, Albazzaz AS, Taufiq-Yap YH. Deoxygenation of waste cooking to renewable diesel over walnut shell-derived nanorode activated carbon supported CaO-La2O3 catalyst. Energy Convers Manag 2017;151:311–23. https://doi.org/10.1016/j.enconman.2017.09.001.

[36] Asikin-Mijan N, Lee HV, Taufiq-Yap YH, Abdulkrem-Alsultan G, Mastuli MS, Ong HC. Optimization study of SiO2-Al2O3 supported bifunctional acid–base NiO-CaO for renewable fuel production using response surface methodology. Energy Convers Manag 2017;141:325–38. https://doi.org/10.1016/j.enconman.2016.09.041.
[37] Hafriz RSRM, Nor Shafizah I, Salmiaton A, Arifin NA, Yunus R, Taufiq Yap YH, Abd Halim S. Comparative study of transition metal-doped calcined Malaysian dolomite catalysts for WCO deoxygenation reaction. Arab J Chem 2020;13:8146–59. https://doi.org/10.1016/j.arabjc.2020.09.046.
[38] Kamil FH, Salmiaton A, Hafriz RSRM, Hussien IR, Omar R. Characterization and application of molten slag as catalyst in pyrolysis of waste cooking oil. Bull Chem Reaction Eng Catal 2020;15:119–27. https://doi.org/10.9767/bcrec.15.1.3973.119-127.
[39] Zhou C, Rosén C, Engvall K. Selection of dolomite bed material for pressurized biomass gasification in BFB. Fuel Process Technol 2017;167:511–23. https://doi.org/10.1016/j.fuproc.2016.11.017.
[40] Harith N, Hafriz RSRM, Arifin NA, Tan ES, Salmiaton A, Shamsuddin AH. Catalytic co-pyrolysis of blended biomass – plastic mixture using synthesized metal oxide (MO)-dolomite based catalyst. J Anal Appl Pyrolysis 2022;168. https://doi.org/10.1016/j.jaap.2022.105776.
[41] Shajaratun Nur ZA, Taufiq-Yap YH, Rabiah Nizah MF, Teo SH, Syazwani ON, Islam A. Production of biodiesel from palm oil using modified Malaysian natural dolomites. Energy Convers Manag 2014;78:738–44. https://doi.org/10.1016/j.enconman.2013.11.012.
[42] Yang H, Dong H, Zhang T, Zhang Q, Zhang G, Wang P, Liu Q. Calcined dolomite: an efficient and recyclable catalyst for synthesis of α, β-unsaturated carbonyl compounds. Catal Lett 2019;149:778–87. https://doi.org/10.1007/s10562-018-2632-9.
[43] Ma X, Li Y, Yan X, Zhang W, Zhao J, Wang Z. Preparation of a morph-genetic CaO-based sorbent using paper fibre as a biotemplate for enhanced CO2 capture. Chem Eng J. 2019;361:235–44. https://doi.org/10.1016/j.cej.2018.12.061.
[44] Feng Long F, Li F, Zhai Q, Wang F, Xu J. Thermochemical conversion of waste acidic oil into hydrocarbon products over basic composite catalysts. J Clean Prod 2019;234:105–12. https://doi.org/10.1016/j.jclepro.2019.06.109.
[45] Li H, Wang Y, Zhou N, Dai L, Deng W, Liu C, Cheng Y, Liu Y, Cobb K, Chen P, Ruan R. Applications of calcium oxide–based catalysts in biomass pyrolysis/gasification – A review. J Clean Prod 2021;291. https://doi.org/10.1016/j.jclepro.2021.125826.
[46] Xu J, Jiang J, Sun Y, Chen J. Production of hydrocarbon fuels from pyrolysis of soybean oils using a basic catalyst. Bioresour Technol 2010;101:9803–6. https://doi.org/10.1016/j.biortech.2010.06.147.
[47] Junming X, Jianchun J, Yanju L, Jie C. Liquid hydrocarbon fuels obtained by the pyrolysis of soybean oils. Bioresour Technol 2009;100:4867–70. https://doi.org/10.1016/j.biortech.2009.04.055.
[48] Stefanidis SD, Karakoulia SA, Kalogiannis KG, Iliopoulou EF, Delimitis A, Yiannoulakis H, Zampetakis T, Lappas AA, Triantafyllidis KS. Natural magnesium oxide (MgO) catalysts: a cost-effective sustainable alternative to acid zeolites for the in situ upgrading of biomass fast pyrolysis oil. Appl Catal B 2016;196:155–73. https://doi.org/10.1016/j.apcatb.2016.05.031.
[49] Ding K, Liu S, Huang Y, Liu S, Zhou N, Peng P, Wang Y, Chen P, Ruan R. Catalytic microwave-assisted pyrolysis of plastic waste over NiO and HY for gasoline-range hydrocarbons production. Energy Convers Manag 2019;196:1316–25. https://doi.org/10.1016/j.enconman.2019.07.001.
[50] Park Y, Kim Y, Chang S. Transition Metal-Catalyzed C-H Amination: scope, mechanism, and applications. Chem Rev 2017;117:9247–301. https://doi.org/10.1021/acs.chemrev.6b00644.
[51] Rahman NJA, Ramli A, Jumbri K, Uemura Y. Tailoring the surface area and the acid–base properties of ZrO2 for biodiesel production from Nannochloropsis sp. Sci Rep 2019;9. https://doi.org/10.1038/s41598-019-52771-9.
[52] Shamsuddin MR, Asikin-Mijan N, Marliza TS, Miyamoto M, Uemiya S, Yarmo MA, Taufiq-Yap YH. Promoting dry reforming of methaneviabifunctional NiO/dolomite catalysts for production of hydrogen-rich syngas. RSC Adv 2021;11:6667–81. https://doi.org/10.1039/d0ra09246k.
[53] Hafriz RSRM, Arifin NA, Salmiaton A, Yunus R, Taufiq-Yap YH, Saifuddin NM, Shamsuddin AH. Multiple-objective optimization in green fuel production via catalytic deoxygenation reaction with NiO-dolomite catalyst. Fuel 2022;308. https://doi.org/10.1016/j.fuel.2021.122041.
[54] Adira Wan Khalit WN, Marliza TS, Asikin-Mijan N, Gamal MS, Saiman MI, Ibrahim ML, Taufiq-Yap YH. Development of bimetallic nickel-based catalysts supported on activated carbon for green fuel production. RSC Adv 2020;10:37218–32. https://doi.org/10.1039/d0ra06302a.
[55] Wang R, Li H, Chang F, Luo J, Hanna MA, Tan D, Hu D, Zhang Y, Song B, Yang S. A facile, low-cost route for the preparation of calcined porous calcite and dolomite and their application as heterogeneous catalysts in biodiesel production. Catal Sci Technol 2013;3:2244–51. https://doi.org/10.1039/c3cy00129f.
[56] M. Hartman, K. Svoboda, J. Kocurek, Decomposition Kinetics of Alkaline-Earth Hydroxides and Surface Area of Their Calcines, n.d.
[57] Wang K, Han D, Zhao P, Hu X, Yin Z, Wu D. Role of MgxCa1-xCO3 on the physical-chemical properties and cyclic CO2 capture performance of dolomite by two-step calcination. Thermochim Acta 2015;614:199–206. https://doi.org/10.1016/j.tca.2015.06.033.
[58] Toncón-Leal CF, Villarroel-Rocha J, Silva MTP, Braga TP, Sapag K. Characterization of mesoporous region by the scanning of the hysteresis loop in adsorption–desorption isotherms. Adsorption 2021;27:1109–22. https://doi.org/10.1007/s10450-021-00342-8.
[59] Safa-Gamal M, Asikin-Mijan N, Arumugam M, Khalit WNAW, Nur Azreena I, Hafez FS, Taufiq-Yap YH. Catalytic deoxygenation by H2-free single-step conversion of free fatty acid feedstock over a Co-Ag carbon-based catalyst for green diesel production. J Anal Appl Pyrolysis 2021;160. https://doi.org/10.1016/j.jaap.2021.105334.
[60] Shafihi U, Hafriz RSRM, Arifin NA, Nor Shafizah I, Idris A, Salmiaton A, Razali NM. Catalytic deoxygenation with SO42–Fe2O3/Al2O3 catalyst: optimization by Taguchi method. Results Eng 2023;17. https://doi.org/10.1016/j.rineng.2023.100959.
[61] Zikri A, Aznury M. Green diesel production from Crude Palm Oil (CPO) using catalytic hydrogenation method. In: IOP Conf Ser Mater Sci Eng. Institute of Physics Publishing; 2020. https://doi.org/10.1088/1757-899X/823/1/012026.
[62] Asikin-Mijan N, Lee HV, Juan JC, Noorsaadah AR, Taufiq-Yap YH. Catalytic deoxygenation of triglycerides to green diesel over modified CaO-based catalysts. RSC Adv 2017;7:46445–60. https://doi.org/10.1039/c7ra08061a.
[63] Hafriz RSRM, Nor Shafizah I, Arifin NA, Maisarah AH, Salmiaton A, Shamsuddin AH. Comparative, reusability and regeneration study of potassium oxide-based catalyst in deoxygenation reaction of WCO. Energy Convers Manag: X 2022;13. https://doi.org/10.1016/j.ecmx.2021.100173.
[64] Jenkins RW, Moore CM, Semelsberger TA, Chuck CJ, Gordon JC, Sutton AD. The effect of functional groups in bio-derived fuel candidates. ChemSusChem 2016;9:922–31. https://doi.org/10.1002/cssc.201600159.
[65] Asikin-Mijan N, Juan JC, Taufiq-Yap YH, Ong HC, Lin YC, AbdulKareem-Alsultan G, Lee HV. Towards sustainable green diesel fuel production: advancements and opportunities in acid-base catalyzed H2-free deoxygenation process. Catal Commun 2023;182. https://doi.org/10.1016/j.catcom.2023.106741.
[66] Hongloi N, Prapainainar P, Prapainainar C. Review of green diesel production from fatty acid deoxygenation over Ni-based catalysts. Mol Catal 2022;523. https://doi.org/10.1016/j.mcat.2021.111696.
[67] Rahmawati Z, Santoso L, McCue A, Azua Jamari NL, Ninglasari SY, Gunawan T, Fansuri H. Selectivity of reaction pathways for green diesel production towards biojet fuel applications. RSC Adv 2023;13:13698–714. https://doi.org/10.1039/d3ra02281a.
[68] Logan TJ, Underwood DC, Rheinecker TC. Hydrolysis of triglycerides. United States Patent; 1980.
[69] Zhang Y, Fan L, Liu S, Zhou N, Ding K, Peng P, Anderson E, Addy M, Cheng Y, Liu Y, Li B, Snyder J, Chen P, Ruan R. Microwave-assisted co-pyrolysis of brown coal and corn stover for oil production. Bioresour Technol 2018;259:461–4. https://doi.org/10.1016/j.biortech.2018.03.078.
[70] Lee MK, Tsai WT, Tsai YL, Lin SH. Pyrolysis of napier grass in an induction-heating reactor. J Anal Appl Pyrolysis 2010;88:110–6. https://doi.org/10.1016/j.jaap.2010.03.003.
[71] Chen G, Liu C, Ma W, Zhang X, Li Y, Yan B, Zhou W. Co-pyrolysis of corn cob and waste cooking oil in a fixed bed. Bioresour Technol 2014;166:500–7. https://doi.org/10.1016/j.biortech.2014.05.090.
[72] J. Donnelly, R. Horton, K. Gopalan, C.D. Bannister, C.J. Chuck, Branched ketone biofuels as blending agents for jet-a1 aviation kerosene, energy and fuels 30 (2016) 294–301. https://doi.org/10.1021/acs.energyfuels.5b01629.
[73] Al Dawery S, AbdulMajeed W, Al Shukaili S, Thotireddy C, Al Amri I. Produced Water Deoxygenation via Nitrogen Purging Scheme– Parametric Study – Part 2. Eng Technol J 2022;40:1–15. https://doi.org/10.30684/etj.2022.134758.1248.
[74] Nirdosh I, Garred LJ, Baird MHI. Low-cost experiments in mass transfer. Part 3. Mass Transfer in a Bubble Column 1998.
[75] Si Z, Zhang X, Wang C, Ma L, Dong R. An overview on catalytic hydrodeoxygenation of pyrolysis oil and its model compounds. Catalysts 2017;7. https://doi.org/10.3390/catal7060169.
[76] Huo X, Xiao J, Song M, Zhu L. Comparison between in-situ and ex-situ catalytic pyrolysis of sawdust for gas production. J Anal Appl Pyrolysis 2018;135:189–98. https://doi.org/10.1016/j.jaap.2018.09.003.
[77] Collard FX, Bensakhria A, Drobek M, Volle G, Blin J. Influence of impregnated iron and nickel on the pyrolysis of cellulose. Biomass Bioenergy 2015;80:52–62. https://doi.org/10.1016/j.biombioe.2015.04.032.
[78] Gao FYJJL. In: Proceedings of 2012 International Conference on Biobase Material Science and Engineering: October 21-23, 2012. Changsha, China: IEEE; 2012.
[79] Yu F, Gao L, Wang W, Zhang G, Ji J. Bio-fuel production from the catalytic pyrolysis of soybean oil over Me-Al-MCM-41 (Me = La, Ni or Fe) mesoporous materials. J Anal Appl Pyrolysis 2013;104:325–9. https://doi.org/10.1016/j.jaap.2013.06.017.
[80] Emori EY, Hirashima FH, Zandonai CH, Ortiz-Bravo CA, Fernandes-Machado NRC, Olsen-Scaliante MHN. Catalytic cracking of soybean oil using ZSM5 zeolite. Catal Today 2017;279:168–76. https://doi.org/10.1016/j.cattod.2016.05.052.
[81] Smoljan CS, Crawford JM, Carreon MA. Mesoporous microspherical NiO catalysts for the deoxygenation of oleic acid. Catal Commun 2020;143. https://doi.org/10.1016/j.catcom.2020.106046.
[82] D. Septriana, M. Mufti Azis, J. Wintoko, EasyChair preprint catalytic decarboxylation of palm oil to green diesel over pellets of Ni-CaO/activated carbon (AC) catalyst in subcritical water catalytic decarboxylation of palm oil to green diesel over pellets of Ni-CaO/Activated Carbon (AC) catalyst under subcritical water, 2021.
[83] Ong HC, Mahlia TMI, Masjuki HH, Honnery D. Life cycle cost and sensitivity analysis of palm biodiesel production. Fuel 2012;98:131–9. https://doi.org/10.1016/j.fuel.2012.03.031.